NASA Contractor Report 187600
ICASE Report No. 91–54

ICASE

THE INVISCID COMPRESSIBLE GÖRTLER PROBLEM

Andrew Dando
Sharon O. Seddougui

Contract No. NAS1–18605
July 1991

Institute for Computer Applications in Science and Engineering
NASA Langley Research Center
Hampton, Virginia 23665–5225

Operated by the Universities Space Research Association

National Aeronautics and
Space Administration

Langley Research Center
Hampton, Virginia 23665-5225

THE INVISCID COMPRESSIBLE GÖRTLER PROBLEM

Andrew Dando[1]
Department of Mathematics
Oxford Road
University of Manchester
Manchester, M13 9PL
United Kingdom

and

Sharon O. Seddougui
Institute for Computer Applications in Science and Engineering
NASA Langley Research Center
Hampton, VA 23665

ABSTRACT

In this paper we investigate the growth rates of Görtler vortices in a compressible flow in the inviscid limit of large Görtler number. Numerical solutions are obtained for 0(1) wavenumbers. The further limits of (i) large Mach number and (ii) large wavenumber with 0(1) Mach number are considered. We show that two different types of disturbance modes can appear in this problem. The first is a wall layer mode, so named as it has its eigenfunctions trapped in a thin layer near the wall. The other mode we investigate is confined to a thin layer away from the wall and termed a trapped layer mode for large wavenumbers and an adjustment layer mode for large Mach numbers, since then this mode has its eigenfunctions concentrated in the temperature adjustment layer. We are able to investigate the near crossing of the modes which occurs in each of the limits mentioned.

[1]This research was supported by the National Aeronautics and Space Administration under NASA Contract No. NAS1-18605 while the authors were in residence at the Institute for Computer Applications in Science and Engineering (ICASE), NASA Langley Research Center, Hampton, VA 23665.

1. Introduction

Our aim in this paper is to investigate the growth rates of Görtler vortices for a compressible inviscid flow over an infinite cylinder in the limits of high Mach number and high wavenumber. This investigation is motivated by recent interest in the development of hypersonic aircraft which might well be capable of reaching speeds in the order of 20 - 25 Mach. Real gas effects will certainly come into play at these speeds but for simplicity's sake we have not taken them into account in this paper. We have also assumed that Chapman's viscosity law holds for this fluid.

The most obvious difference between Görtler vortices in incompressible and hypersonic flows is that the presence of a temperature adjustment layer, where the temperature decays rapidly to its free stream value, at the edge of the boundary layer enables hypersonic Görtler vortices to be concentrated well away from the wall. In the incompressible case, we know, from the work of Hall (1982a,b, 1983), and Denier, Hall, and Seddougui (1991), that unstable Görtler vortices are not localized within the boundary layer for order one Görtler numbers. For higher Görtler numbers the most dangerous Görtler vortices have wavelengths small compared to the boundary layer thickness and are trapped near the wall. Not surprisingly this situation does not change significantly for order one Mach numbers and this nonparallel problem has been discussed by Wadey (1990) and Spall and Malik (1989). In the latter two papers, the nonparallel equations were solved numerically following the approach of Hall (1983) and the main result obtained was that the growth rate of a Görtler vortex is a function of its upstream history. The numerical calculations of Wadey (1990) do suggest that as the Mach number increases the unstable Görtler vortices locate themselves towards the edge of the boundary layer. This view is supported by Hall and Fu (1989) whose main result was that the logarithmically small temperature adjustment layer at the edge of a hypersonic boundary layer can support Görtler vortices and the most dangerous wavelengths of the vortices are comparable with the thickness of this layer. Fu, Hall, and Blackaby (1990) have considered the influence of real gas effects and Sutherland's viscosity law on the Görtler instability in hypersonic flows.

This present paper is restricted to linear regimes of vortex growth, for a detailed account of nonlinear regimes the reader is referred to the review article by Hall (1990). It is also worth noting that hypersonic boundary layers are susceptible to instabilities other than those caused by streamline curvature, such as Tollmien-Schlichting wave instabilities which have been discussed by Cowley and Hall (1990) and Smith and Brown (1990). Clearly any nonlinear investigation of Görtler vortices at hypersonic speeds must allow for the possible interaction of the vortices and these other types of instabilities.

The present paper is concerned with the inviscid limit of Görtler vortices in a compressible

boundary layer. We find that two distinct modes exist and we are able to describe them in the separate limits of large free-stream Mach number and large disturbance wavenumber (although for the case of large free-stream Mach number the disturbance wavenumber will also be large). The first mode also exists in an incompressible boundary layer and is termed a wall layer mode here since its eigenfunctions are concentrated in a thin layer near to the wall. For the incompressible case, in the limit of large wavenumber, this mode is described by Denier, Hall, and Seddougui (1991). The second mode has its eigenfunctions concentrated in a thin layer away from the wall and therefore is referred to as a trapped layer mode in the large wavenumber limit. In the hypersonic limit this layer is precisely the temperature adjustment layer, a logarithmic layer where the basic temperature changes rapidly from its $O(M_\infty^2)$ value close to the wall to its 0(1) value at the edge of the boundary layer. Consequently, in the hypersonic limit this mode is termed an adjustment layer mode.

The numerical solution of the equations governing the stability of Görtler vortices in the inviscid limit, discussed in Section 2, show that the growth rates of the infinity of solutions of the two modes described above, as functions of the disturbance wavenumber, appear to intersect. A similar near-crossing of modes is evident in the numerical results of Mack (1987) in the form of kinks in the neutral curves of the generalized inflection point modes for compressible flow over a flat plate. Asymptotic solutions for the infinity of solutions of the compressible Rayleigh equation, termed acoustic modes, in the hypersonic limit have been given by Cowley and Hall (1990), while the so-called, single, vorticity mode for large values of the Mach number has been discussed by Smith and Brown (1990). Cowley and Hall (1990) postulated that the near-crossing of the neutral curves could be described by a WKB description of the acoustic modes and the vorticity mode. This is precisely the method employed by Smith and Brown (1990) in their investigation of inviscid modes of instability for large Mach number flows. The results of Smith and Brown (1990) show that the discontinuous vorticity mode becomes continuous in the limit of large Mach number. Additionally, they ascertain that for large Mach numbers the acoustic and vorticity modes are separated by an exponentially small amount as was proposed by Cowley and Hall (1990).

The objective of the present paper is to describe the wall layer modes and trapped layer modes present for inviscid Görtler vortices and to investigate their near-crossing which exists as outlined above. To this aim we follow the ideas of Cowley and Hall (1990) and Smith and Brown (1990) and consider a WKB analysis of the modes of interest.

The layout of this paper is as follows. In Section 2 we derive the equation governing the structure of inviscid Görtler vortices in a compressible boundary layer and then discuss some numerical results of this equation. In Section 3 we take a closer look at the wall layer modes, those with their eigenfunctions trapped near the wall, in the hypersonic limit. We follow

this by looking at the adjustment layer modes, those whose eigenfunctions are concentrated in the temperature adjustment layer, in the hypersonic limit in Section 4. Then in Section 5 we look at the wall layer modes for the high wavenumber limit. In Section 6 we consider the trapped layer modes for the high wavenumber limit, these are the equivalent of the adjustment layer modes for the hypersonic limit. We then consider the near crossing of the different types of modes for both limits in Section 7 before finally summarizing our results in Section 8.

2. Formulation

Our aim in this section is to obtain the equation which determines the structure of a Görtler vortex in a compressible boundary layer. The boundary layer considered is that of a flow over the cylinder $y^* = 0, -\infty < z^* < \infty$ so that the z^*-axis is a generator of the cylinder and y^* measures the distance normal to the surface. The x^*-coordinate measures distance along the curved surface, which is supposed to have variable curvature $(1/m)\chi(x^*/l)$ where m and l are length scales. The Reynolds number R, Görtler number G and curvature parameter δ^* are defined by

$$R = \frac{U_\infty l}{\nu}, \tag{2.1a}$$

$$G = 2R^{\frac{1}{2}}\delta^*, \tag{2.1b}$$

$$\delta^* = \frac{l}{m}, \tag{2.1c}$$

where U_∞ is a typical flow velocity in the streamwise direction and ν is the kinematic viscosity of the fluid. The Reynolds number is assumed to be large, whilst δ^* is sufficiently small so that as $\delta^* \to 0$ the parameter G is fixed and of order one. We take the basic two-dimensional boundary layer to be of the form

$$\underline{u} = U_\infty[\overline{u}(X,Y), R^{-\frac{1}{2}}\overline{v}(X,Y), 0][1 + O(R^{-\frac{1}{2}})], \tag{2.2}$$

where

$$X = \frac{x^*}{l}, \quad Y = \frac{y^* R^{\frac{1}{2}}}{l}. \tag{2.3}$$

We chose to look at a Blasius boundary layer by putting $\overline{u} = f'(\eta)$ where f satisfies

$$2f''' + ff'' = 0, \; f(0) = f'(0) = 0, \; f'(\infty) = 1, \tag{2.4}$$

and η is given by

$$\eta = Y^*/X^{\frac{1}{2}}, \tag{2.5}$$

where Y^* is the Howarth-Dorodnitsyn variable

$$Y^* = \int_0^Y \frac{1}{\overline{T}} dY, \tag{2.6}$$

and we have taken a model fluid (i.e., the Prandtl number equal to one and Chapman's viscosity law with C equal to one). For the case of a thermally insulating wall, the temperature is given by

$$\overline{T} = 1 + \frac{1}{2}(\gamma - 1)M_\infty^2(1 - f'^2), \tag{2.7}$$

where M_∞ is the Mach number of the free stream and γ is the ratio of the specific heats and will be taken to be 1.4 when it is needed numerically. Defining Z by

$$Z = \frac{z^* R^{\frac{1}{2}}}{l}, \tag{2.8}$$

we perturb (2.2) by writing

$$\underline{u} = U_\infty[\overline{u} + \delta\hat{U}(X,Y)E_1,\ \overline{v}R^{-\frac{1}{2}} + \delta R^{-\frac{1}{2}}\hat{V}(X,Y)E_1,\ \delta R^{-\frac{1}{2}}\hat{W}(X,Y)E_1][1 + O(R^{-\frac{1}{2}})], \tag{2.9}$$

where $E_1 = \exp(iaZ)$ and $\delta \ll 1$ (see Hall (1982a) for further discussion of the above scalings). We similarly perturb the basic pressure, $\overline{p}$, by putting

$$p = \overline{p} + \delta R^{-1}\hat{P}(X,Y)E_1, \tag{2.10}$$

and the basic temperature by

$$\tilde{T} = T_\infty(\overline{T} + \delta\hat{T}(X,Y)E_1), \tag{2.11}$$

where T_∞ is the free stream temperature. If we then introduce a growth rate $\hat{\beta}$ and the scalings

$$\hat{U}(X,Y) = U(Y)E_2, \tag{2.12a}$$

$$\hat{V}(X,Y) = G^{\frac{1}{2}}V(Y)E_2, \tag{2.12b}$$

$$\hat{W}(X,Y) = G^{\frac{1}{2}}W(Y)E_2, \tag{2.12c}$$

$$\hat{T}(X,Y) = T(Y)E_2, \tag{2.12d}$$

$$\hat{P}(X,Y) = GP(Y)E_2, \tag{2.12e}$$

where

$$E_2 = \exp\left\{\int G^{\frac{1}{2}}\hat{\beta}(X)dX\right\}, \tag{2.12f}$$

and insert (2.9) - (2.11) into the governing equations and take the inviscid limit $G \to \infty$ we get

$$\frac{\overline{p}\hat{\beta}U}{\overline{T}} + \frac{\partial}{\partial Y}\left(\frac{\overline{p}V}{\overline{T}}\right) + \frac{ia\overline{p}}{\overline{T}}W - \frac{\hat{\beta}\overline{p}\ \overline{u}T}{\overline{T}^2} = 0, \tag{2.13a}$$

$$\overline{u}\hat{\beta}U + V\frac{\partial \overline{u}}{\partial Y} = 0, \tag{2.13b}$$

$$\frac{\overline{p}}{\overline{T}}\left[\overline{u}\hat{\beta}V + K\overline{u}U\right] - \frac{1}{2}\frac{\overline{p}\,\overline{u}^2 KT}{\overline{T}^2} = -\frac{\partial P}{\partial Y}, \tag{2.13c}$$

$$\frac{\overline{p}\,\overline{u}\hat{\beta}}{\overline{T}}W = -iaP, \tag{2.13d}$$

$$\overline{u}\hat{\beta}T + V\frac{\partial \overline{T}}{\partial Y} = 0, \tag{2.13e}$$

where K is a measure of the curvature. Taking $\overline{p} = 1$ we find from (2.13) that

$$V\left[\frac{Ka^2}{2\hat{\beta}\overline{u}}\frac{\partial}{\partial Y}\left(\frac{\overline{u}^2}{\overline{T}}\right) - \frac{\hat{\beta}a^2\overline{u}}{\overline{T}} - \frac{\partial}{\partial Y}\left(\frac{\hat{\beta}}{\overline{T}}\frac{\partial \overline{u}}{\partial Y}\right)\right] + \hat{\beta}\overline{u}\frac{\partial}{\partial Y}\left(\frac{1}{\overline{T}}\frac{\partial V}{\partial Y}\right) = 0. \tag{2.14}$$

If we now change variables to η, take for simplicity's sake a value of $X = 1$ and put

$$\hat{\beta} = K^{\frac{1}{2}}\beta, \tag{2.15}$$

in order to eliminate K from the equation we get after some rearranging

$$V'' + V'\left[-\frac{2\overline{T}'}{\overline{T}}\right] + V\left[\left(-a^2\overline{T}^2 - \frac{f'''}{f'} + \frac{2\overline{T}'}{\overline{T}}\frac{f''}{f'}\right) + \frac{a^2}{\beta^2}\left(\overline{T}\frac{f''}{f'} - \frac{\overline{T}'}{2}\right)\right] = 0, \tag{2.16}$$

with the boundary conditions

$$V(0) = 0, \tag{2.17a}$$

$$V \sim e^{-a\eta} \quad \text{as} \quad \eta \to \infty, \tag{2.17b}$$

$$V' \sim -ae^{-a\eta} \quad \text{as} \quad \eta \to \infty. \tag{2.17c}$$

Since (2.16) corresponds to an inviscid limit we cannot satisfy the viscous boundary condition $V' = 0$ at $\eta = 0$. Equation (2.16) is the compressible generalization of equation (5.8) in Denier, Hall, and Seddougui (1991). Similarly to Denier, Hall, and Seddougui (1991) it can be seen that (2.16) and (2.17) have the exact solution

$$V = f'e^{-a\eta}, \quad \beta^2 = \frac{a}{2}, \tag{2.18}$$

which is valid for all a and M_∞. However, in order to get other solutions it is necessary to solve this eigenvalue problem numerically.

We solved (2.16) and (2.17) for a variety of Mach numbers. Figure 1 shows the first eleven modes for a Mach number of 2. These modes are not markedly different in shape from those of the form $\beta^2 =$ constant $\times\, a$ obtained in the incompressible case (again, see Denier, Hall, and Seddougui (1991)). Figure 2 shows solutions for a Mach number of 3.25 and we can see that there are now significant differences compared with the incompressible

case. However, all of the modes continue to rise as $a \to \infty$ and are of the wall layer type, so-called because the eigenfunction is concentrated in a layer near the wall. In Figure 3 where the Mach number is now 5, we can clearly see the appearance of two adjustment layer modes which tend to a constant value of β as $a \to \infty$. We call these modes adjustment layer modes because their eigenfunctions are concentrated in the temperature adjustment layer in the hypersonic limit. (They will be referred to as trapped layer modes for 0(1) Mach numbers.) Each of the modes in this figure (apart from the exact solution) contributes a portion to the adjustment layer modes as they pass through the relevant positions and in doing so they change up to the next higher wall layer mode. If we follow the fourth mode on Figure 3 as a increases we can look at its eigenfunction and see how it changes. Initially when $a = 0.2$ we can see in Figure 4a that the eigenfunction is a widened version of the eigenfunction of the third wall layer mode with an additional lower peak in the temperature adjustment layer. In Figure 4b with $a = 1.1$ the mode is now in its flat section and the eigenfunction is indeed that of an adjustment layer mode. By the time $a = 1.25$, Figure 4c shows that the peak in the temperature adjustment layer has split into two. In Figure 4d we have $a = 1.35$ and the left-hand peak of these twin peaks is moving into the wall layer whilst the right-hand peak is decaying, showing the process by which the modes change up to the next higher wall layer mode. To complete the sequence, Figure 4e shows the eigenfunction for $a = 2.5$ and it turns out to be the eigenfunction of the fourth wall layer mode.

Figure 5 shows solutions for a Mach number of 8 and we can see the first three adjustment layer modes. As the Mach number and wavenumber increase, the modes come very close to intersecting (although they do not as we shall show in Section 7) and this means we have to take prohibitively small steps in a in order to follow a particular mode numerically. As a result, some wall layer type portions of modes have been omitted from Figure 5.

3. The Wall Layer Modes for $M_\infty \gg 1$

Taking Equation (2.16) and using the scalings

$$a = \frac{\overline{a}}{M_\infty^2} + \cdots, \tag{3.1}$$

and

$$\beta = \frac{\overline{\beta}}{M_\infty} + \cdots, \tag{3.2}$$

allows us to look at the wall layer modes for $M_\infty \gg 1$, for which

$$V'' + V'\left[\frac{4f'f''}{(1-f'^2)}\right] + V\left[\left(-\frac{1}{4}\overline{a}^2(\gamma-1)^2(1-f'^2)^2 - \frac{f'''}{f'}\right.\right.$$
$$\left.\left. - \frac{4f''^2}{(1-f'^2)}\right) + \frac{1}{2}(\gamma-1)\frac{\overline{a}^2}{\overline{\beta}^2}\left(\frac{f''}{f'}(1-f'^2) + f'f''\right)\right] = 0. \tag{3.3}$$

When $\overline{a} \gg 1$ we can get an approximation to the wall layer modes by the application of the WKB method. There are three regions to consider as we have a turning point associated with the WKB expansion. Close to the wall the transformation

$$V(\eta) = S(\eta)(1-f'^2), \tag{3.4}$$

allows us to write (3.3) as

$$S''(1-f'^2) - 2S(f'f'' + f''^2 + f'f''') + S(1-f'^2)\left[\left(-\frac{1}{4}\overline{a}^2(\gamma-1)^2(1-f'^2)^2\right.\right.$$
$$\left.\left. - \frac{f'''}{f'} - \frac{4f''^2}{(1-f'^2)}\right) + \frac{1}{2}(\gamma-1)\frac{\overline{a}^2}{\overline{\beta}^2}\left(\frac{f''}{f'}(1-f'^2) + f'f''\right)\right] = 0, \tag{3.5}$$

which for $\overline{a} \gg 1$ gives the WKB approximation

$$S'' + \overline{a}^2 S\left[-\frac{1}{4}(\gamma-1)^2(1-f'^2) + \frac{1}{2}\frac{(\gamma-1)}{\overline{\beta}^2}\left(\frac{f''}{f'}(1-f'^2) + f'f''\right)\right] = 0, \tag{3.6}$$

and we write this as

$$S'' + \overline{a}^2 S H(\eta, \overline{\beta}) = 0, \tag{3.7}$$

where

$$H = -\frac{1}{4}(\gamma-1)^2(1-f'^2) + \frac{1}{2}\frac{(\gamma-1)}{\overline{\beta}^2}\left(\frac{f''}{f'}(1-f'^2) + f'f''\right),$$

$H > 0$ for $0 \leq \eta < \eta_t$ and η_t is the turning point. In order to satisfy the boundary condition (2.17a) we must have $S(0) = 0$ since $(1-f') \neq 0$ for $\eta = 0$. The solution of (3.7) which satisfies $S(0) = 0$ is

$$S(\eta) = \frac{A}{H^{\frac{1}{4}}}\sin(\overline{a}\int_0^\eta (H(\eta_1))^{\frac{1}{2}} d\eta_1), \tag{3.8}$$

where A is a constant and so V is given by

$$V = \frac{A(1-f'^2)}{H^{\frac{1}{4}}}\sin(\overline{a}\int_0^\eta (H(\eta_1))^{\frac{1}{2}} d\eta_1). \tag{3.9}$$

In the region of the turning point, the equation to be solved is the Airy equation

$$V'' - \overline{a}^2\sigma(\eta - \eta_t)V = 0, \tag{3.10}$$

where σ is positive and given by

$$\sigma = -\left.\frac{dH}{d\eta}\right|_{\eta=\eta_t}. \tag{3.11}$$

The required solution of (3.10) which decays exponentially as $\eta \to \infty$ is

$$V = B\pi^{\frac{1}{2}} Ai([\overline{a}^2\sigma]^{\frac{1}{3}}(\eta - \eta_t)), \tag{3.12}$$

where B is a constant and Ai denotes the Airy function (see Abramowitz and Stegun (1964)). If we denote the argument of the Airy function by t then since for $t \ll -1$

$$Ai(t) \sim \pi^{-\frac{1}{2}}|t|^{-\frac{1}{4}} \sin\left(\frac{2}{3}|t|^{\frac{3}{2}} + \frac{\pi}{4}\right), \tag{3.13}$$

we have that for $t \ll -1$

$$V \approx \frac{B}{|t|^{\frac{1}{4}}} \sin\left(\frac{2}{3}|t|^{\frac{3}{2}} + \frac{\pi}{4}\right). \tag{3.14}$$

Now letting $\eta \to \eta_t$ in (3.9) gives

$$V = \frac{A(1 - f'(\eta_t)^2)}{\sigma^{\frac{1}{4}}(\eta_t - \eta)^{\frac{1}{4}}} \sin(\overline{a}\int_0^{\eta_t} (H(\eta_1))^{\frac{1}{2}} d\eta_1). \tag{3.15}$$

Matching amplitudes and phases between (3.14) and (3.15) implies, since we allow B to be positive or negative in (3.12) and hence phases may be either in phase or π radians out of phase, that

$$\frac{A(1 - f'(\eta_t)^2)\overline{a}^{\frac{1}{6}}}{\sigma^{\frac{1}{6}}} = \pm B, \tag{3.16}$$

and

$$\overline{a} = \frac{n\pi - \frac{\pi}{4}}{J_-}, \tag{3.17}$$

where

$$J_- = \int_0^{\eta_t} (H(\eta_1))^{\frac{1}{2}} d\eta_1, \tag{3.18}$$

and n is a large integer.

In Figure 6 we have plotted the wall layer modes, with equation (3.17) for n running from one through seven and a Mach number of 8, and then superimposed them on Figure 5. We can see, even for a moderate Mach number and small values of n, that equation (3.17) gives a good approximation to the wall layer modes.

4. The Adjustment Layer Modes for $M_\infty \gg 1$

For the adjustment layer modes, the appropriate equation below the turning point is (3.9). However, (3.12), the solution of the Airy equation (3.10), must now be replaced by

$$V = E\pi^{\frac{1}{2}} Ai(t) + F\pi^{\frac{1}{2}} Bi(t), \tag{4.1}$$

where E and F are constants since V will be large in the temperature adjustment layer away from the wall and so we are no longer seeking a solution which decays exponentially beyond the turning point. Thus for $t \ll -1$, since

$$Bi(t) \sim \pi^{-\frac{1}{2}}|t|^{-\frac{1}{4}} \cos\left(\frac{2}{3}|t|^{\frac{3}{2}} + \frac{\pi}{4}\right), \tag{4.2}$$

we have

$$V \approx \frac{(E^2+F^2)^{\frac{1}{2}}}{|t|^{\frac{1}{4}}} \sin\left(\frac{2}{3}|t|^{\frac{3}{2}} + \frac{3\pi}{4} - \phi\right), \tag{4.3}$$

where $\tan\phi = E/F$. Matching (3.9) and (4.3) gives

$$\frac{A(1-f'(\eta_t)^2)\overline{a}^{\frac{1}{6}}}{\sigma^{\frac{1}{6}}} = \pm(E^2+F^2)^{\frac{1}{2}}, \tag{4.4}$$

and

$$\overline{a} = \frac{n\pi - \frac{3\pi}{4} + \phi}{J_-}, \tag{4.5}$$

where n is again a large integer.

When $t \gg 1$ we have

$$Ai(t) = \frac{1}{2}\pi^{-\frac{1}{2}}t^{-\frac{1}{4}}\exp(-\frac{2}{3}t^{\frac{3}{2}}), \tag{4.6}$$

and

$$Bi(t) = \pi^{-\frac{1}{2}}t^{-\frac{1}{4}}\exp\left(\frac{2}{3}t^{\frac{3}{2}}\right), \tag{4.7}$$

so (4.1) gives for $t \gg 1$ that

$$V \approx Ft^{-\frac{1}{4}}\exp\left(\frac{2}{3}t^{\frac{3}{2}}\right), \tag{4.8}$$

and this has to be matched with the solution above the turning point but below the temperature adjustment layer. In this region V is given by

$$V \approx \frac{c_0(1-f'^2)}{(-H)^{\frac{1}{4}}}\exp(\overline{a}\int_{\eta_t}^{\eta}(-H(\eta_1))^{\frac{1}{2}}d\eta_1), \tag{4.9}$$

where we have only retained the exponentially large term, multiplied by a constant c_0, in the WKB approximation. Matching between (4.8) and (4.9) gives

$$\frac{F}{c_0} = \frac{\overline{a}^{\frac{1}{6}}}{\sigma^{\frac{1}{6}}}(1-(f'(\eta_t))^2). \tag{4.10}$$

The temperature adjustment layer has $z = 0(1)$ where

$$\eta = b + \Gamma - \left(\frac{\log\Gamma + z}{\Gamma}\right), \tag{4.11}$$

and b is a constant and

$$\Gamma = \sqrt{2\log(M_\infty^2)}. \tag{4.12}$$

In this region therefore

$$f' \approx 1 - \frac{he^z}{M_\infty^2}, \tag{4.13}$$

where h is a constant so

$$\overline{T} \approx 1 + (\gamma - 1)he^z, \tag{4.14}$$

and hence

$$-H \approx \frac{(\gamma-1)^2 h^2 e^{2z}}{M_\infty^4} - \frac{\frac{1}{2}(\gamma-1)}{\overline{\beta}^2}\frac{he^z\Gamma}{M_\infty^2}. \tag{4.15}$$

Therefore if we take $z \gg 1$ and insert these expansions into (4.9) we get that the behavior of V as the temperature adjustment layer is entered from below is

$$V \approx \frac{2c_0 h^{\frac{1}{2}}}{M_\infty(\gamma-1)^{\frac{1}{2}}} e^{\frac{1}{2}z} \exp\left\{\overline{a}J_+ - \frac{\overline{a}}{\Gamma}\frac{(\gamma-1)he^z}{M_\infty^2}\right\}, \tag{4.16}$$

where

$$J_+ = \int_{\eta_t}^{\infty} \left[\frac{1}{4}(\gamma-1)^2(1-f'^2) - \frac{1}{2}\frac{(\gamma-1)}{M_\infty^2\beta^2}\left(\frac{f''}{f'}(1-f'^2) + f'f''\right)\right]^{\frac{1}{2}} d\eta. \tag{4.17}$$

In the temperature adjustment layer we make the transformation (4.11) in (2.16) and after scaling a and β by writing

$$a = \tilde{a}\Gamma + \ldots, \tag{4.18a}$$

$$\beta = \tilde{\beta}\Gamma^{\frac{1}{2}} + \ldots, \tag{4.18b}$$

we get, retaining the leading order terms for $M_\infty \gg 1$, that

$$\frac{d^2V}{dz^2} + \frac{dV}{dz}\left[\left(\frac{1-(\gamma-1)he^z}{1+(\gamma-1)he^z}\right) - 1\right] + V\tilde{a}^2\left[-(1+(\gamma-1)he^z)^2 + \frac{1}{\tilde{\beta}^2}\left(\frac{(\gamma-1)he^z}{2}\right)\right] = 0. \tag{4.19}$$

From (4.16) we can see that as $z \to \infty$ the behavior of V will be a multiple of

$$s^{\frac{1}{2}}e^{-\tilde{a}s}, \tag{4.20}$$

where

$$s = (\gamma-1)he^z. \tag{4.21}$$

Letting $z \to -\infty$ in (4.19) we can easily see that

$$V \sim e^{\tilde{a}z}, \tag{4.22}$$

since we require V to decay above the temperature adjustment layer. Using (4.20) and (4.22) as boundary conditions we solved (4.19) numerically. In Figure 7 we have plotted the first three adjustment layer modes given by (4.19) for a Mach number of 8 and superimposed

this onto Figure 5. We can see that (4.19) is giving a good approximation to the adjustment layer modes.

The numerical results we gained in Section 2 seemed to suggest the existence of a critical Mach number, above which the adjustment layer modes come into play and below which they do not exist, and we shall discuss this further in Section 6.

5. The Wall Layer Modes for $M_\infty \sim 0(1)$

The modes located near the wall for $M_\infty \sim 0(1)$ will be described by Equation (2.16). For large a we are able to obtain an approximation to them from the WKB solution in a similar way to the solution obtained in Section 3 in the hypersonic limit.

If we write

$$\beta = \beta^+ a^{\frac{1}{2}}, \tag{5.1}$$

then there is no turning point in the WKB solution. However, the solution obtained does breakdown when $\eta \sim 0(a^{-1})$ as a consequence of $f' \sim \alpha\eta$ for $\eta \ll 1$. Thus, in this region we write

$$\psi = aT_w\eta, \tag{5.2}$$

where T_w is the value of $\overline{T}(\eta)$ at $\eta = 0$. (When the flow is adiabatic, i.e., the wall is thermally insulating, from (2.7), $T_w = 1 + (\gamma - 1)M_\infty^2/2$.) Substituting (5.1) and (5.2) into (2.16) we find that V satisfies the following equation:

$$-\beta^{+2}\left(\frac{d^2V}{d\psi^2} - V\right) = \frac{V}{\psi}. \tag{5.3}$$

This is the equation satisfied by V in the corresponding incompressible problem described by Denier, Hall, and Seddougui (1991). It is a form of Whittaker's equation and the solution for V satisfying the boundary conditions

$$V = 0 \text{ at } \psi = 0,$$

and

$$V \to 0 \text{ as } \psi \to \infty,$$

may be given in terms of Kummer functions (see Abramowitz and Stegun 1964). Hence, we find that the unstable eigenvalues for the present case of a compressible fluid will be the same as those for the incompressible problem described by Denier, Hall, and Seddougui (1991). These are

$$\sqrt{2}\beta^+ = 1, \frac{1}{\sqrt{2}}, \frac{1}{\sqrt{3}}, \cdots .$$

Thus from (5.1) the growth rates for the wall layer modes are given by

$$\beta^2 = \frac{a}{2n}, \tag{5.4}$$

where $n = 1, 2, 3, \ldots$. We note that the first solution corresponds to the exact solution described by (2.18). Moreover, the eigenvalues are independent of M_∞ and T_w.

The appropriate solution of (5.3) is

$$V(\psi) = b_1 e^{-\psi} \psi M(1-n, 2, 2\psi), \tag{5.5}$$

where $M(a, b, z)$ is Kummer's function and b_1 is a constant. $M(1-n, 2, 2\psi)$ is a polynomial of degree $(n-1)$ in 2ψ. The behavior of V for large ψ is

$$V(\psi) \sim b_1 (-1)^{n-1} \frac{2^{n-1}}{n!} e^{-\psi} \psi^n + \ldots . \tag{5.6}$$

Then from (2.16), we find that the WKB solution in the region above the wall layer which matches with (5.6) as $\eta \to 0$ is given by

$$V(\eta) = c_1 (\overline{T}(\eta))^{(1-n)/2} (f'(\eta))^n \exp[-a \int_0^\eta \overline{T}(\eta_1) d\eta_1], \tag{5.7}$$

where c_1 is a constant. Since

$$f'(\eta) \sim \alpha\eta - \frac{\alpha^2}{48}\eta^4 + \ldots, \tag{5.8}$$

for $\eta \ll 1$, where $\alpha = 0.332\ldots$, c_1 is given by

$$c_1 = a^n T_w^{(3n-1)/2} \alpha^{-n} (-1)^{n-1} \frac{2^{n-1}}{n!} b_1. \tag{5.9}$$

In Figure 8 we show the growth rate given by (5.4) as a function of a for $M_\infty = 5$ for the first nine wall modes. These solutions are superimposed on the corresponding numerical solutions from Section 2. We see that for large a the asymptotic results are very good approximations to the numerical solutions.

In order to discuss the near-linking of these wall layer modes and the trapped layer modes described in the next section, we must consider the solution of the wall layer modes for large mode number. This is apparent from Figure 3 since the growth rates of the wall layer modes will not be close to those of the trapped layer modes for $a \gg 1$ unless n is large.

Thus for $n \gg 1$ we write the wavenumber as

$$a = a_0 n + a_1 + \ldots, \tag{5.10}$$

where a_0 and a_1 are constants. Then from (5.4) the growth rate of the wall layer modes for large n is given by

$$\beta = \frac{a_0^{\frac{1}{2}}}{2^{\frac{1}{2}}} + \frac{a_1}{8^{\frac{1}{2}} a_0^{\frac{1}{2}} n} + \dots . \tag{5.11}$$

From (5.5) the solution for V in the wall layer for large n is

$$V(\psi) = b_1 2^{-\frac{3}{4}} \pi^{-\frac{1}{2}} n^{-\frac{3}{4}} \psi^{\frac{1}{4}} \cos\left(8^{\frac{1}{2}} \psi^{\frac{1}{2}} n^{\frac{1}{2}} - \frac{3\pi}{4}\right). \tag{5.12}$$

As $\psi \to 0$ the solution (5.12) matches onto the solution in a thin layer next to the wall of thickness $0(n^{-1})$ where V satisfies

$$\frac{d^2V}{d\zeta^2} + \frac{2V}{\zeta} = 0, \tag{5.13}$$

and $\zeta = n\psi$. To satisfy the boundary condition at the wall and to match with (5.12) as $\zeta \to \infty$ we find that

$$V \sim e_1(\zeta - \zeta^2 + \dots) \quad \text{for } \zeta \ll 1,$$

and

$$V \sim b_1 2^{-\frac{3}{4}} \pi^{-\frac{1}{2}} n^{-1} \zeta^{\frac{1}{4}} \cos\left(8^{\frac{1}{2}} \zeta^{\frac{1}{2}} - \frac{3\pi}{4}\right) \quad \text{as } \zeta \to \infty,$$

where e_1 is a constant.

For large values of ψ the solution given by (5.12) is valid only for $\psi < 2n$ and matches onto the solution above the wall layer for large n when ψ is large and $\psi < 2n$. We find that the WKB solution in the region above the wall layer which matches with (5.12) as $\eta \to 0$ is given by

$$V(\eta) = g_1(-Q(\eta))^{-\frac{1}{4}} \overline{T}(\eta) \cos((na_0 + a_1) \int_0^\eta (-Q)^{\frac{1}{2}} d\eta_1 - \frac{a_1}{2a_0} \int_0^\eta \left(\frac{\overline{T}^2}{(-Q)^{\frac{1}{2}}} + (-Q)^{\frac{1}{2}}\right) d\eta_1 - \theta_1), \tag{5.14}$$

where g_1 is a constant and $\theta_1 = 3\pi/4$. The function $Q(\eta)$ is defined by

$$Q(\eta) = (\overline{T}(\eta))^2 - \frac{2}{a_0}\left(\frac{\overline{T}(\eta) f''(\eta)}{f'(\eta)} - \frac{\overline{T}'(\eta)}{2}\right), \tag{5.15}$$

and the solution (5.14) is valid for $0 < \eta < \eta^*$ where η^* is the first zero of Q and $Q < 0$ for $\eta < \eta^*$. A more thorough discussion of the function Q is given in the next section.

In the region close to $\eta = \eta^*$, from (2.16) V satisfies

$$V'' - \tau(\eta - \eta^*) a_0^2 n^2 V = 0, \tag{5.16}$$

where $\tau = Q'(\eta^*) > 0$. Since we require V to decay as $\eta \to \infty$ the appropriate solution of (5.16) is

$$V = k_0 \pi^{\frac{1}{2}} Ai(r), \tag{5.17}$$

where k_0 is a constant and $r = (a_0^2 n^2 \tau)^{\frac{1}{3}}(\eta - \eta^*)$. From the behavior of the Airy function Ai given by (3.13) for $r \to -\infty$ we have from (5.17) that

$$V \sim k_0 |r|^{-\frac{1}{4}} \cos\left(\frac{2}{3}|r|^{\frac{3}{2}} - \frac{\pi}{4}\right), \tag{5.18}$$

as $r \to -\infty$. Then matching the amplitudes and phases of (5.14) as $\eta \to \eta^*$ with (5.18) gives

$$\tau^{-\frac{1}{4}}(a_0^2 n^2 \tau)^{\frac{1}{12}} \overline{T}(\eta^*) g_1 = k_0, \tag{5.19a}$$

and

$$(na_0 + a_1) I_1 - \frac{a_1}{2a_0}(I_1 + I_2) - \theta_1 = \frac{\pi}{4}, \tag{5.19b}$$

where the integrals I_1 and I_2 are defined by

$$I_1 = \int_0^{\eta^*} (-Q)^{\frac{1}{2}} d\eta_1, \tag{5.20a}$$

and

$$I_2 = \int_0^{\eta^*} \overline{T}^2 (-Q)^{-\frac{1}{2}} d\eta_1. \tag{5.20b}$$

The expression (5.19b) determines a_1, i.e.,

$$a_1 = \frac{\theta_1 + \frac{\pi}{4} - na_0 I_1}{I_1 - \frac{1}{2a_0}(I_1 + I_2)}. \tag{5.21}$$

6. The Trapped Layer Mode for $M_\infty \sim 0(1)$

For $M_\infty \sim 0(1)$ this mode is concentrated away from the wall and is the equivalent of the temperature adjustment layer made for $M_\infty \gg 1$ described in Section 4. For $a \gg 1$ this mode can be regarded as a virtually continuous function of a. In Section 7.2, we discuss the near-linking of this mode with the wall layer solution for large n. Anticipating this we define a by (5.10) and consider the solution of the trapped layer mode for $n \gg 1$. To obtain the solution for large a from the following results we set $a_1 = 0$ and $a_0 n = a$. For large n we write (2.16) in the form

$$V'' - 2\frac{\overline{T}'}{\overline{T}} V' - a_0^2 n^2 Q V = 0, \tag{6.1}$$

where

$$Q(\eta) = \overline{T}^2 \left[1 - \frac{1}{\beta^2}\left(\frac{f''}{\overline{T} f'} - \frac{\overline{T}'}{2\overline{T}^2}\right)\right] \tag{6.2}$$

Then this mode is concentrated in the region where

$$\beta^2 = \beta_0^2 = \left(\frac{f''}{\overline{T} f'} - \frac{\overline{T}'}{2\overline{T}^2}\right)\Bigg|_{\eta = \tilde{\eta}}, \tag{6.3}$$

and β is a maximum at $\eta = \tilde{\eta}$. Therefore, from (6.2) we have

$$Q(\tilde{\eta}) = Q'(\tilde{\eta}) = 0 \quad \text{and} \quad Q''(\tilde{\eta}) > 0. \tag{6.4}$$

Thus when $a_0 = 2\beta_0^2$ the function Q defined by (6.2) is also that defined by (5.15).

In Figure 9 we plot $Q(\eta)/\overline{T}^2$ from (6.2) for $M_\infty = 5$ for a range of values of β. We choose to show $Q/\overline{T}^2$ rather than Q since $(\overline{T}(\eta))^2$ given by (2.7) is large for small values of η and decays exponentially to the free stream value of 1 as η increases. We see from Figure 9 that $Q(\eta) \to -\infty$ as $\eta \to 0+$. For certain values of β the function $Q(\eta)$ has three zeros. For a particular value of β the second and third zeros coincide in a turning point. This position of η is the location of the trapped layer modes $\eta = \tilde{\eta}$, for large a. The sequence of modes will be described by corrections to (6.3).

However, these trapped modes will not exist for values of M_∞ below a critical value. We can see this if we look at the plots of $Q(\eta)/\overline{T}^2$ for various values of β for $M_\infty = 3$ shown in Figure 10. It is apparent from this figure that $Q(\eta)$ only has one zero for any value of β and no local minimum for $M_\infty = 3$. For the Chapman constant $C = 1$ and an adiabatic fluid the critical value of M_∞ is found to be $M_\infty = M_c = 3.564$. Thus, for $M_\infty < M_c$ the function Q will not have a local minimum and there is no solution described by (6.3) and (6.4). This explains why the discontinuous modes do not appear in the computational results for small Mach numbers. We note that there exists a critical value of the free stream Mach number when $C \neq 1$ or Prandtl number $\neq 1$ and also for the case of an isothermal flow where the temperature of the wall is maintained at a constant value.

Thus, from (6.3) β is a constant to first order for the trapped modes and moreover, the same constant for each mode. The correction to β will describe the distinct modes. In order to determine the eigenfunction in this region it is necessary to determine the correction to β. In the trapped layer

$$\hat{\eta} = a_0^{\frac{1}{2}} n^{\frac{1}{2}} (\eta - \tilde{\eta}), \tag{6.5}$$

where $\hat{\eta} \sim 0(1)$. Write

$$\beta = \beta_0 + a_0^{-1} n^{-1} \beta_1 + \ldots, \tag{6.6}$$

and substitute (6.5) and (6.6) into (6.1). Equating coefficients of the largest terms, which are of $0(a_0^2 n^2)$, shows that β_0 is indeed defined by (6.3) and (6.4).

Figures 11 and 12 show the solutions of (6.3) and (6.4) for an adiabatic fluid and also for the case of an isothermal fluid where the temperature of the wall is maintained at a constant value. In this case for Chapman constant $C = 1$ and a Prandtl number of unity, the basic temperature is given by

$$\overline{T}(\eta) = 1 + \frac{\gamma - 1}{2} M_\infty^2 (f'(\eta) - f'(\eta))^2) + (T_w - 1)(1 - f'(\eta)), \tag{6.7}$$

where T_w is the nondimensional temperature of the wall. Note that if $T_w = 1+(\gamma-1)M_\infty^2/2$ then (6.7) reduces to the expression (2.7) for an adiabatic flow.

Figure 11 shows the value of $\tilde{\eta}$ for the trapped modes as a function of Mach number for an adiabatic wall and an isothermal wall with $T_w = 0.5,\ 1,\ 2,\ 4,\ 8$. We see that $\tilde{\eta}$ moves towards the free stream as M_∞ increases. For large values of M_∞ the analysis must be replaced with that described in Section 4 so $\tilde{\eta}$ will correspond to the position of the temperature adjustment layer given by (4.11) and the modes will be as described in Section 4. This is consistent with (4.11) since we see that the position of the temperature adjustment layer increases as M_∞ increases.

Figure 12 shows the corresponding values of β_0 for the trapped modes as a function of Mach number. We see for the adiabatic case and for the isothermal case with $T_w < 8$ that the value of β_0 decreases initially as M_∞ increases but then increases as M_∞ increases further.

The $0(a_0 n)$ terms in (6.1) give the following equation for V:

$$\frac{d^2V}{d\hat{\eta}^2} - \frac{Q''(\tilde{\eta})}{2}\hat{\eta}^2 V - \frac{2\beta_1}{\beta_0}(\overline{T}(\tilde{\eta}))^2 V = 0, \tag{6.8}$$

where $Q''(\tilde{\eta})$ is defined for $\beta = \beta_0$. The solution of (6.8) satisfying the boundary conditions

$$V \to 0 \text{ as } |\hat{\eta}| \to \infty, \tag{6.9}$$

is an eigenvalue problem for β_1. We find that the solution of (6.8) and (6.9) is

$$V(\overline{\eta}) = d_1 U(\lambda, \overline{\eta}), \tag{6.10}$$

where d_1 is a constant,

$$\overline{\eta} = (2Q''(\tilde{\eta}))^{\frac{1}{4}}\hat{\eta}, \tag{6.11}$$

$$\lambda = \frac{2^{\frac{1}{2}}(\overline{T}(\tilde{\eta}))^2\beta_1}{(Q''(\tilde{\eta}))^{\frac{1}{2}}\beta_0}, \tag{6.12}$$

and $U(\lambda, \overline{\eta})$ is the Parabolic cylinder function (see Abramowitz and Stegun 1964). Now $U(\lambda, \overline{\eta})$ grows exponentially as $\overline{\eta} \to -\infty$ unless

$$\lambda = -\frac{1}{2},\ -\frac{3}{2},\ -\frac{5}{2}, \cdots \ . \tag{6.13}$$

Then the behavior of $U(\lambda, \overline{\eta})$ as $\overline{\eta} \to -\infty$ when λ is given by (6.13) is

$$U(\lambda, \overline{\eta}) \sim (-1)^{-\lambda-\frac{1}{2}}|\overline{\eta}|^{-\lambda-\frac{1}{2}}e^{-\overline{\eta}^2/4}, \tag{6.14}$$

and

$$U(\lambda, \overline{\eta}) \sim \overline{\eta}^{-\lambda-\frac{1}{2}}e^{-\overline{\eta}^2/4}, \tag{6.15}$$

as $\overline{\eta} \to +\infty$.

From (6.12) and (6.13) we can evaluate β_1 for a fixed Mach number for a particular trapped mode. Figure 13 shows the growth rate from (6.6) for $M_\infty = 5$ for the first three trapped modes as a function of a. In order to see the comparison between the numerical solution of the discontinuous mode described in Section 2, in Figure 13 only the discontinuous solutions are shown for large a and β below a certain value. We see from Figure 13 that for the first trapped layer mode the asymptotic solution is a very good agreement even for 0(1) values of a. For successive modes we still have good agreement but for larger values of a.

Below $\eta = \tilde{\eta}$, but above $\eta = \eta^*$ where $Q(\eta^*) = 0$, $Q(\eta)$ will be positive. The WKB solution of (2.16) in the region $\eta^* < \eta < \tilde{\eta}$ is

$$V(\eta) = e_0(Q(\eta))^{-\frac{1}{4}}\overline{T}(\eta)\exp\left[\left(a_0 n + a_1 - \frac{\beta_1}{\beta_0}\right)\int_{\eta^*}^{\eta} Q^{\frac{1}{2}}d\eta_1 + \frac{\beta_1}{\beta_0}\int_{\eta^*}^{\eta}\overline{T}^2 Q^{-\frac{1}{2}}d\eta_1\right], \tag{6.16}$$

where e_0 is a constant. Now as $\eta \to \tilde{\eta}$

$$\int_{\eta^*}^{\eta} Q^{\frac{1}{2}}d\eta_1 \sim \int_{\eta^*}^{\tilde{\eta}} Q^{\frac{1}{2}}d\eta_1 - a_0^{-1}n^{-1}\frac{\overline{\eta}^2}{4}, \tag{6.17}$$

and

$$\frac{\beta_1}{\beta_0}\int_{\eta^*}^{\eta}\overline{T}^2 Q^{-\frac{1}{2}}d\eta_1 \sim \frac{\beta_1}{\beta_0}\int_{\eta^*}^{\tilde{\eta}-(a_0 n)^{-\frac{1}{2}}}\overline{T}^2 Q^{-\frac{1}{2}}d\eta_1 - \lambda\ ln((2Q''(\tilde{\eta}))^{-\frac{1}{4}}|\overline{\eta}|), \tag{6.18}$$

where λ satisfies (6.12). Thus, from (6.16) as $\eta \to \tilde{\eta}$ for large n

$$V \sim 2^{\frac{3}{8}}a_0^{\frac{1}{4}}n^{\frac{1}{4}}(Q''(\tilde{\eta}))^{-\frac{1}{8}}\overline{T}(\tilde{\eta})e_0|\overline{\eta}|^{-\lambda-\frac{1}{2}}(2Q'')^{\frac{\lambda}{4}}\exp\left[-\frac{\overline{\eta}^2}{4} + \left(a_0 n + a_1 - \frac{\beta_1}{\beta_0}\right)I_3 + I_4\right], \tag{6.19}$$

where I_3 and I_4 are integrals defined by

$$I_3 = \int_{\eta^*}^{\tilde{\eta}} Q^{\frac{1}{2}}d\eta, \tag{6.20a}$$

and

$$I_4 = \frac{\beta_1}{\beta_0}\int_{\eta^*}^{\tilde{\eta}-(a_0 n)^{-\frac{1}{2}}}\overline{T}^2 Q^{-\frac{1}{2}}d\eta. \tag{6.20b}$$

Then (6.19) matches with (6.10) as $\overline{\eta} \to -\infty$ if

$$2^{\frac{3}{8}}a_0^{\frac{1}{4}}n^{\frac{1}{4}}(Q''(\overline{\eta}))^{-\frac{1}{8}}\overline{T}(\tilde{\eta})(2Q'')^{\frac{\lambda}{4}}e_0\exp\left[\left(a_0 n + a_1 - \frac{\beta_1}{\beta_0}\right)I_3 + I_4\right] = d_1(-1)^{-\lambda-\frac{1}{2}}. \tag{6.21}$$

Close to the position $\eta = \eta^*$ V satisfies (5.16). We do not require V to decay above this region so the solution for V is

$$V = k_0\pi^{\frac{1}{2}}Ai(r) + l_0\pi^{\frac{1}{2}}Bi(r), \tag{6.22}$$

where k_0 and l_0 are constants.

From (4.8) the behavior of V as $r \to \infty$ is

$$V \sim l_0 r^{-\frac{1}{4}} \exp\left(\frac{2}{3} r^{\frac{3}{2}}\right). \tag{6.23}$$

The solution (6.16) must match with (6.23) as $\eta \to \eta^*$. Then l_0 is given by

$$l_0 = e_0 \tau^{-\frac{1}{4}} (a_0^2 n^2 \tau)^{\frac{1}{12}} \overline{T}(\eta^*). \tag{6.24}$$

From (6.22) as $r \to -\infty$

$$V \sim (k_0^2 + l_0^2)^{\frac{1}{2}} |r|^{-\frac{1}{4}} \cos\left(\frac{2}{3}|r|^{\frac{3}{2}} + \frac{\pi}{4} - \theta_2\right), \tag{6.25}$$

where $\tan\theta_2 = k_0/l_0$. In the region below $\eta = \eta^*$ V is given by (5.14), i.e., the solution above the wall layer for $n \gg 1$. Thus matching the solution (5.14) as $\eta \to \eta^*$ with (6.25) gives instead of (5.19)

$$\tau^{-\frac{1}{4}} (a_0^2 n^2 \tau)^{\frac{1}{12}} \overline{T}(\eta^*) g_1 = \pm (k_0^2 + l_0^2)^{\frac{1}{2}}, \tag{6.26}$$

and

$$(n a_0 + a_1) I_1 - \frac{a_1}{2a_0}(I_1 + I_2) - \theta_1 = \theta_2 - \frac{\pi}{4}. \tag{6.27}$$

7. The Near Crossing of the Wall Layer and Adjustment Layer Modes

We see from the numerical results of Section 2 that for values of the free stream Mach number above a critical 0(1) value the wall layer modes and the adjustment layer modes become very close. This occurs for 0(1) values of the wavenumber and continues to occur as the wavenumber increases.

A similar near crossing occurs for the inflectional acoustic neutral modes and the vorticity mode associated with the inviscid instability of a Blasius boundary layer for a compressible fluid and was discussed by Cowley and Hall (1990) and Smith and Brown (1990). The latter authors confirmed the conjecture of the former that, in the hypersonic limit, the modes are separated by an exponentially small amount.

To discuss the near crossing of the two different types of mode described in Sections 3 and 4 for $M_\infty \gg 1$ and in Sections 5 and 6 for $a \gg 1$ we follow Smith and Brown (1990) and extend our WKB analysis of these previous sections.

Since the near crossing occurs for 0(1) Mach numbers as well as for $M_\infty \gg 1$ it should be possible to discuss the near crossing for both situations. The analysis will be similar for each case and therefore we attempt to minimize any repetition. We will first discuss the situation for the hypersonic limit.

7.1. The Hypersonic Limit

We again have that below the turning point V is given by (3.9). In the region of the turning point V is given by (4.1) and (4.3) - (4.5) still hold. However, we replace (4.8) by

$$V \approx \frac{1}{t^{\frac{1}{4}}}\left[\frac{1}{2}E\exp\left(-\frac{2}{3}t^{\frac{3}{2}}\right) + F\exp\left(\frac{2}{3}t^{\frac{3}{2}}\right)\right], \tag{7.1}$$

for $t \gg 1$. We also retain the exponentially small term in (4.9) so that V in the region between the turning point and the temperature adjustment layer is given by

$$V \approx \frac{(1-f'^2)}{(-H)^{\frac{1}{4}}}\left[c_0\exp\left\{\overline{a}\int_{\eta_t}^{\eta}(-H(\eta_1))^{\frac{1}{2}}d\eta_1\right\} + d_0\exp\left\{-\overline{a}\int_{\eta_t}^{\eta}(-H(\eta_1))^{\frac{1}{2}}d\eta_1\right\}\right]. \tag{7.2}$$

We already have (4.10) and matching the exponentially small terms between (7.1) and (7.2) gives

$$\frac{E}{2d_0} = \frac{\overline{a}^{\frac{1}{6}}}{\sigma^{\frac{1}{6}}}(1-f'(\eta_t)^2), \tag{7.3}$$

so that

$$\frac{E}{2d_0} = \frac{F}{c_0}. \tag{7.4}$$

We now need to augment (4.16), the behavior as the temperature adjustment layer is approached from below, by a corresponding term in d_0 so that

$$V \approx \frac{2h^{\frac{1}{2}}}{M_\infty(\gamma-1)^{\frac{1}{2}}}e^{\frac{1}{2}z}\left[c_0\exp\left\{\overline{a}J_+ - \frac{\overline{a}}{\Gamma}\frac{(\gamma-1)h}{M_\infty^2}e^z\right\} + d_0\exp\left\{-\overline{a}J_+ + \frac{\overline{a}}{\Gamma}\frac{(\gamma-1)h}{M_\infty^2}e^z\right\}\right], \tag{7.5}$$

and then match this with the behavior of V in the temperature adjustment layer as $z \to \infty$.

If we assume (4.19) has a solution

$$V = \overline{V}, \tag{7.6a}$$

$$\tilde{a} = \overline{A}, \tag{7.6b}$$

$$\tilde{\beta} = \overline{B}, \tag{7.6c}$$

and then perturb these equations by putting

$$V = \overline{V} + \tilde{V}, \tag{7.7a}$$

$$\tilde{a} = \overline{A} + \tilde{A}, \tag{7.7b}$$

$$\tilde{\beta} = \overline{B} + \tilde{B}, \tag{7.7c}$$

and insert (7.7) into (4.19) we get after linearising

$$\frac{d^2\tilde{V}}{dz^2}+\frac{d\tilde{V}}{dz}\left[\left(\frac{1-(\gamma-1)he^z}{1+(\gamma-1)he^z}\right)-1\right]+\tilde{V}\overline{A}^2\left[-(1+(\gamma-1)he^z)^2+\frac{1}{\overline{B}^2}\left(\frac{(\gamma-1)he^z}{2}\right)\right]$$

$$=\overline{V}\left[2\overline{A}\tilde{A}(1+(\gamma-1)he^z)^2+\left(\frac{\overline{A}^2\tilde{B}}{\overline{B}^3}-\frac{\overline{A}\tilde{A}}{\overline{B}^2}\right)(\gamma-1)he^z\right], \tag{7.8}$$

which can be integrated to give

$$\tilde{V}=\overline{V}w(z), \tag{7.9}$$

with

$$w(z)=2\overline{A}\tilde{A}\int_0^z\left(\frac{[1+(\gamma-1)he^{z_1}]^2}{\overline{V}^2}\int_0^{z_1}\overline{V}^2dz_2\right)dz_1$$

$$+\left(\frac{\overline{A}^2\tilde{B}}{\overline{B}^3}-\frac{\overline{A}\tilde{A}}{\overline{B}^2}\right)(\gamma-1)h\int_0^z\left(\frac{[1+(\gamma-1)he^{z_1}]^2}{\overline{V}^2}\int_0^{z_1}\frac{e^{z_2}\overline{V}^2}{[1+(\gamma-1)he^{z_2}]^2}dz_2\right)dz_1 \tag{7.10}$$

$$+\frac{C_1}{(\gamma-1)h}\int_0^z\frac{[1+(\gamma-1)he^{z_1}]^2}{\overline{V}^2}dz_1+C_2.$$

Using (4.22) we can calculate the constant C_1 that is necessary to ensure that $\tilde{V}$ decays exponentially as $z\to-\infty$. We can then use (4.20) to calculate the behavior of $w(z)$ as $z\to\infty$ and if we choose C_2 so that there is no additional contribution of order $s^{\frac{1}{2}}e^{-\tilde{a}s}$ to V from $\tilde{V}$ then we have that as $z\to\infty$, V goes as

$$V\sim[(\gamma-1)he^z]^{\frac{1}{2}}\left[\exp\{-\overline{A}(\gamma-1)he^z\}+\right.$$

$$\left.\left(-\tilde{A}C_3-\left(\frac{\overline{A}\tilde{B}}{\overline{B}^3}-\frac{\tilde{A}}{\overline{B}^2}\right)\frac{(\gamma-1)h}{2}C_4\right)\exp\{\overline{A}(\gamma-1)he^z\}\right], \tag{7.11}$$

where

$$C_3=\int_0^{-\infty}\overline{V}^2dz-\int_0^{\infty}\overline{V}^2dz, \tag{7.12}$$

and

$$C_4=\int_0^{-\infty}\frac{e^z\overline{V}^2}{[1+(\gamma-1)he^z]^2}dz-\int_0^{\infty}\frac{e^z\overline{V}^2}{[1+(\gamma-1)he^z]^2}dz. \tag{7.13}$$

Matching between (7.5) and (7.11) gives us that

$$\frac{c_0}{d_0}=-\left[\tilde{A}C_3+\left(\frac{\overline{A}\tilde{B}}{\overline{B}^3}-\frac{\tilde{A}}{\overline{B}^2}\right)\frac{(\gamma-1)h}{2}C_4\right]^{-1}\exp\{-2\overline{a}J_+\}, \tag{7.14}$$

so we can get F/E from (7.4). Assuming F is small since we want to perturb the wall layer modes (as well as the adjustment layer modes) for which F is zero, we get

$$\phi \approx \frac{\pi}{2} - \frac{F}{E}, \tag{7.15}$$

and inserting this into (4.5) gives after some rearranging

$$\begin{aligned} &\left(a - \frac{n\pi - \frac{\pi}{4}}{M_\infty^2 J_-}\right)\left(a - \Gamma\left[\overline{A} + \frac{\overline{A}\tilde{B}(\gamma-1)hC_4}{(\gamma-1)hC_4\overline{B} - 2C_3\overline{B}^3}\right]\right) \\ &\qquad = \frac{\overline{B}^2\Gamma}{2C_3\overline{B}^2 - (\gamma-1)hC_4} \cdot \frac{\exp\{-2aM_\infty^2 J_+\}}{M_\infty^2 J_-}. \end{aligned} \tag{7.16}$$

Setting the two brackets equal to zero gives respectively the wall layer modes and the adjustment layer modes. We can see from (7.16) that for finite M_∞ these modes do not intersect but the distance between them is exponentially small. This explains the difficulties we had in following a particular mode when we solved (2.16) - (2.17) numerically. A sketch is given in Figure 14 of a pair of these near crossings with the continuous lines representing the situation at a finite Mach number. The dashed lines represent the picture given by (7.16) with the exponentially small right-hand side ignored, i.e., when the adjustment layer modes have become continuous in the limit $M_\infty \to \infty$.

7.2. $M_\infty \sim 0(1)$

As discussed in Section 5, in order to describe the near-linking of the wall layer modes and the trapped layer modes for $M_\infty \sim 0(1)$ we must consider the situation when the mode number of the wall layer mode is large. Similarly to the case when $M_\infty \gg 1$ we extend the WKB analysis of Sections 5 and 6 for $n \gg 1$.

The solution in the wall layer for V is given by (5.12) with the solution below the position $\eta = \eta^*$ given by (5.14). The solution close to $\eta = \eta^*$ is given by (6.22) and so (6.26) and (6.27) are still satisfied.

Now as $r \to \infty$, from (6.22) we replace (6.23) by

$$V \sim r^{-\frac{1}{4}}\left[\frac{k_0}{2}\exp\left(-\frac{2}{3}r^{\frac{3}{2}}\right) + l_0\exp\left(\frac{2}{3}r^{\frac{3}{2}}\right)\right]. \tag{7.17}$$

In the region $\eta^* < \eta < \tilde{\eta}$ we must retain the exponentially decaying term so instead of (6.16)

we have

$$V(\eta) = (Q(\eta))^{-\frac{1}{4}}\overline{T}(\eta)\left\{e_0\exp\left[\left(na_0+a_1-\frac{\beta_1}{\beta_0}\right)\int_{\eta^*}^{\eta}Q^{\frac{1}{2}}d\eta_1+\frac{\beta_1}{\beta_0}\int_{\eta^*}^{\eta}\overline{T}^2Q^{-\frac{1}{2}}d\eta_1\right]\right.$$
$$\left.+h_0\exp\left[-\left(na_0+a_1-\frac{\beta_1}{\beta_0}\right)\int_{\eta^*}^{\eta}Q^{\frac{1}{2}}d\eta_1-\frac{\beta_1}{\beta_0}\int_{\eta^*}^{\eta}\overline{T}^2Q^{-\frac{1}{2}}d\eta_1\right]\right\}, \tag{7.18}$$

where h_0 is a constant. Matching this solution as $\eta \to \eta^*$ with (7.17) gives (6.24) as well as

$$\frac{k_0}{2l_0} = \frac{h_0}{e_0}. \tag{7.19}$$

Following (6.19), from (7.18) as $\eta \to \tilde{\eta}$ for n large

$$V \sim 2^{\frac{3}{8}}a_0^{\frac{1}{4}}n^{\frac{1}{4}}(Q''(\tilde{\eta}))^{-\frac{1}{8}}\overline{T}(\tilde{\eta})\left\{e_0|\overline{\eta}|^{-\lambda-\frac{1}{2}}(2Q''(\tilde{\eta}))^{\frac{\lambda}{4}}\exp\left[-\frac{\overline{\eta}^2}{4}+\left(a_0n+a_1-\frac{\beta_1}{\beta_0}\right)I_3+I_4\right]\right.$$
$$\left.+h_0|\overline{\eta}|^{\lambda-\frac{1}{2}}(2Q''(\tilde{\eta}))^{-\frac{\lambda}{4}}\exp\left[\frac{\overline{\eta}^2}{4}-\left(a_0n+a_1-\frac{\beta_1}{\beta_0}\right)I_3-I_4\right]\right\}. \tag{7.20}$$

Now we make the transformation (6.5) and perturb the solution in the trapped layer for large n where a is given by (5.10). Thus we write

$$\beta = \beta_0 + \frac{1}{a_0n}(\beta_1+\beta^*)+\ldots, \tag{7.21}$$

and

$$V = V_0 + V^*, \tag{7.22}$$

where β^* and V^* are small perturbations and V_0 satisfies (6.8). Then if we substitute (7.21) and (7.22) into (2.16) and linearize about the perturbed quantities we find that V^* satisfies

$$\frac{d^2V^*}{d\hat{\eta}^2}-\frac{Q''(\tilde{\eta})}{2}\hat{\eta}^2V^*-\frac{2\beta_1}{\beta_0}(\overline{T}(\tilde{\eta}))^2V^* = \frac{2\beta^*}{\beta_0}(\overline{T}(\tilde{\eta}))^2V_0. \tag{7.23}$$

We wish to determine the behavior of $V = V_0 + V^*$ as $\hat{\eta} \to -\infty$. We want $V^*(\hat{\eta})$ to decay as $\hat{\eta} \to \infty$ so that the disturbance does not propagate outside the boundary layer. The solution of (7.23) is

$$V^*(\hat{\eta}) = \Psi(\hat{\eta})V_0(\hat{\eta}), \tag{7.24}$$

where $\Psi(\hat{\eta})$ is given by

$$\Psi(\hat{\eta}) = \frac{2\beta^*}{\beta_0}(\overline{T}(\tilde{\eta}))^2\int_0^{\hat{\eta}}\frac{1}{(V_0(\hat{\eta}_1))^2}\int_0^{\hat{\eta}_1}(V_0(\hat{\eta}_2))^2d\hat{\eta}_2d\hat{\eta}_1+D_1\int_0^{\hat{\eta}}\frac{d\hat{\eta}_1}{(V_0(\hat{\eta}_1))^2}+D_2. \tag{7.25}$$

Using the behavior of V_0 as $\hat{\eta} \to \pm\infty$ given by (6.15) and (6.14) we can determine the values of the constants D_1 and D_2. Then from (6.15), since V^* must decay for large $\hat{\eta}$ we find

$$D_1 = -\frac{2\beta^*}{\beta_0}(\overline{T}(\tilde{\eta}))^2(2Q''(\tilde{\eta}))^{-\frac{1}{4}}d_1^2\int_0^\infty (U(\lambda,\overline{\eta}))^2 d\overline{\eta}. \tag{7.26}$$

For $\hat{\eta} \to -\infty$ we choose D_2 to cancel the constant terms. Thus, from (6.14) we find that

$$\Psi(\overline{\eta}) \sim D_3|\overline{\eta}|^{2\lambda}\exp(\overline{\eta}^2/2), \tag{7.27}$$

as $\overline{\eta} \to -\infty$ where

$$D_3 = -(2Q''(\tilde{\eta}))^{-\frac{1}{4}}\left[\frac{2\beta^*}{\beta_0}(\overline{T}(\tilde{\eta}))^2\int_0^{-\infty}(U(\lambda,\overline{\eta}))^2 d\overline{\eta}(2Q''(\tilde{\eta}))^{-\frac{1}{4}} + \frac{D_1}{d_1^2}\right]. \tag{7.28}$$

Thus from (7.26), (7.28) is

$$D_3 = \frac{4\beta^*}{\beta_0}(2Q''(\tilde{\eta}))^{-\frac{1}{2}}(\overline{T}(\tilde{\eta}))^2 I_5, \tag{7.29a}$$

where

$$I_5 = \int_0^\infty (U(\lambda,\overline{\eta}))^2 d\overline{\eta}. \tag{7.29b}$$

Thus, from (7.22), (7.24), (7.27), and (6.14), the behavior of V as $\hat{\eta} \to -\infty$ is given by

$$V(\overline{\eta}) \sim d_1(-1)^{-\lambda-\frac{1}{2}}[|\overline{\eta}|^{-\lambda-\frac{1}{2}}\exp(-\overline{\eta}^2/4) + D_3|\overline{\eta}|^{\lambda-\frac{1}{2}}\exp(\overline{\eta}^2/4)]. \tag{7.30}$$

The WKB solution below the trapped layer must match with (7.30) as $\overline{\eta} \to -\infty$. Thus matching (7.20) and (7.30) gives

$$\frac{e_0}{h_0} = \frac{(2Q''(\tilde{\eta}))^{-\frac{\lambda}{2}}}{D_3}\exp[-2(na_0 + a_1 - \frac{\beta_1}{\beta_0})I_3 - 2I_4]. \tag{7.31}$$

Thus, from (7.19) we have l_0/k_0. The solution for V described above is also a perturbation of the wall layer solution so we must have from (6.22) that l_0 is small. Then we have

$$\theta_2 \sim \frac{\pi}{2} - \frac{l_0}{k_0}. \tag{7.32}$$

Substituting this in (6.27) gives

$$a_1(I_1 - \frac{1}{2a_0}(I_1 + I_2)) + na_0I_1 - \theta_1 - \frac{\pi}{4} = -\frac{l_0}{k_0}. \tag{7.33}$$

Using (7.19) and (7.31) we can rearrange (7.33) to give

$$a_1 = \frac{\theta_1 + \frac{\pi}{4} - na_0I_1}{I_1 - \frac{1}{2a_0}(I_1 + I_2)} - \frac{(2Q''(\tilde{\eta}))^{-\frac{\lambda}{2}}\exp[-2(na_0 + a_1 - \frac{\beta_1}{\beta_0})I_3 - 2I_4]}{2D_3(I_1 - \frac{1}{2a_0}(I_1 + I_2))}. \tag{7.34}$$

Now from (5.11)

$$\beta - \frac{a_0^{\frac{1}{2}}}{2^{\frac{1}{2}}} = \frac{a_1}{8^{\frac{1}{2}} a_0^{\frac{1}{2}} n}. \tag{7.35}$$

Substituting the expression for a_1 from (7.34) into (7.35) and rearranging gives

$$\left[\beta - \frac{a_0^{\frac{1}{2}}}{2^{\frac{1}{2}}} - \frac{1}{8^{\frac{1}{2}} a_0^{\frac{1}{2}} n}\left(\frac{\theta_1 + \pi/4 - n a_0 I_1}{I_1 - \frac{1}{2a_0}(I_1 + I_2)}\right)\right]\left(\beta - \beta_0 - \frac{\beta_1}{a_0 n}\right)$$

$$= \frac{-(2Q''(\tilde{\eta}))^{-\frac{\lambda}{2}} \beta_0 (2Q''(\tilde{\eta}))^{\frac{1}{2}}}{8^{\frac{3}{2}} a_0^{\frac{1}{2}} n (\overline{T}(\tilde{\eta}))^2 I_5 (I_1 - \frac{1}{2a_0}(I_1 + I_2))} \exp\left[-2\left(n a_0 + a_1 - \frac{\beta_1}{\beta_0}\right) I_3 - 2I_4\right]. \tag{7.36}$$

If we set the factors on the left-hand side of (7.36) to zero in turn we see that they describe the growth rates of the wall layer modes and the trapped layer modes respectively. Thus from (7.36) we see that for large n the wall layer modes and the trapped layer modes are separated by an exponentially small amount. This explains the apparent crossings of the growth rate curves obtained from the numerical results of Section 2. Thus the curve of growth rate as a function of a where the modes are very close is also described by Figure 14 as for the case when $M_\infty \gg 1$.

8. Discussion

The main result of the present paper is that we are able to investigate the linear growth rate of Görtler vortices for 0(1) wavenumbers. This was achieved by considering the inviscid limit of large Görtler number for vortices having $0(G^{\frac{1}{2}})$ growth rates. In this limit the growth of Görtler vortices is governed by parallel flow effects. Since for incompressible flows, or compressible flows with 0(1) Mach numbers, the spatial growth of viscous Görtler vortices is governed by non-parallel effects previous investigators were forced to consider the limit of large wavenumber, where as a result of boundary layer growth, non-parallel effects are unimportant (see Hall 1982a and Hall and Malik 1987). However, Hall and Fu (1989) show that in the hypersonic limit the growth of Görtler vortices with wavelength $0((2\log M_\infty^2)^{-\frac{1}{2}})$ is governed by a parallel flow theory.

We have shown that in the inviscid limit, in a compressible boundary layer over an infinite cylinder, there are two types of growth rate modes possible for Görtler vortices.

In the hypersonic limit we have firstly the type of mode we call wall layer modes. These are present in the incompressible case and their growth rates continue to rise as the wavenumber $a \to \infty$. Secondly, we have the adjustment layer modes which have their eigenfunctions concentrated in the temperature adjustment layer away from the wall. The growth rate of these modes tends to a constant value as $a \to \infty$.

We have also considered the limit $a \to \infty$ for 0(1) Mach numbers to describe the wall layer modes and the trapped layer modes (equivalent to the temperature adjustment layer modes when $M_\infty \gg 1$). The wall layer modes are confined to a thin layer of thickness $0(a^{-1})$ and have growth rates proportional to $a^{\frac{1}{2}}$ for moderate mode number n and tending to a constant value for large n. These results are the extension for compressible flows of the incompressible case described in Section 5 of Denier, Hall, and Seddougui (1991), hereafter referred to as DHS. For the compressible case we have an additional mode concentrated in a layer of thickness $0(a^{-\frac{1}{2}})$ away from the wall. This is the so-called "trapped layer mode," which has growth rates tending to a constant value as $a \to \infty$.

The asymptotic results described for $M_\infty \gg 1$ and also for $M_\infty \sim 0(1)$ are shown to agree very well with the numerical solutions described in Section 2. We find that as the Mach number is increased from zero the wall layer modes start to deform until at a critical Mach number we see the appearance of adjustment layer modes.

These modes are not present in an incompressible fluid. However, the growth rate of these modes tends to a constant value as the wavenumber increases while that of the wall layer modes (also present in incompressible flows) continues to increase. Hence, we anticipate that the trapped layer modes will not be as important as the wall layer modes for large values of the wavenumber.

The situation here is similar to the case of inviscid disturbances to compressible flow over a flat plate. In this instance the vorticity mode does not appear until M_∞ exceeds a value approximately given by 2.2. However, in contrast to the present problem, the vorticity mode has larger growth rates than the acoustic modes when $M_\infty \gg 1$.

From the analysis for $a \gg 1$ for Chapman constant $C = 1$ and unit Prandtl number for an adiabatic boundary condition on the basic temperature we find that this critical Mach number is 3.564. For Mach numbers of this range, the adjustment layer modes are discontinuous with each mode solution of (2.16), apart from the exact solution, contributing a part to the adjustment layer modes as it passes through the relevant positions.

We showed in Section 7.1 that for $M_\infty \gg 1$ the wall layer solutions and temperature adjustment layer solutions of (2.16) come within an exponentially small distance of one another and in the hypersonic limit the adjustment layer modes become continuous. In Section 7.2 we showed that this is also the situation in the limit $a \to \infty$ for $M_\infty \sim 0(1)$ when the mode number of the wall layer modes is large.

The Chapman viscosity law has been assumed in the present analysis, and results described for unit Chapman constant and unit Prandtl number for simplicity. There is no great difficulty in obtaining results for more realistic values of C and Prandtl number and it is expected that the effect of this on the asymptotics will be small.

However, in the hypersonic limit the Chapman viscosity law does not give a realistic description of the viscosity of the fluid. Thus, of interest would be the results when the more accurate relation Sutherland's law is used to describe the temperature dependence of the fluid viscosity. The results of Fu, Hall, and Blackaby (1990) who investigated the Görtler instability in the hypersonic limit for Sutherland's law showed that the results were significantly different from those for Chapman's law. In particular the structure of the temperature adjustment layer is altered, now having 0(1) thickness. See also, Blackaby, Cowley, and Hall (1990) who investigated hypersonic flows over a flat plate using Sutherland's law. Thus, it is to be expected that significant changes to the results presented in this paper would exist if Sutherland's viscosity law was used in place of Chapman's law.

The solutions of the equations governing the instability of Görtler vortices in the inviscid limit do not predict a fastest growing mode since the growth rates of the wall layer modes tend to infinity when $a \to \infty$. From Section 5, in the high wavenumber limit we see that the wall layer modes have growth rates of $0(G^{\frac{1}{2}}a^{\frac{1}{2}})$. We can extend the work of DHS to describe the fastest growing mode in the limit of large Görtler number for a compressible flow with $M_\infty \sim 0(1)$. First we consider the structure of a viscous mode close to the right-hand branch of the neutral curve with $a = \lambda^* G^{\frac{1}{4}}$. This mode exists in a layer of thickness $0(a^{-\frac{1}{2}})$ centered around some non-zero value of η. Initially λ^* is 0(1) but we are interested in the limit $\lambda^* \to 0$. We note that the problem where $\lambda^* \to \infty$ corresponds to the work of Hall and Malik (1989). The analysis is very similar to that described by DHS for the corresponding problem for an incompressible problem so the details will not be repeated here. As for the inviscid modes the growth rates are $0(G^{\frac{1}{2}})$. The first approximation to the growth rate $\hat{\beta}$ is determined from the following condition

$$\left(\frac{\overline{u}\hat{\beta}}{\overline{T}} + \overline{\mu}\lambda^{*2}\right)^2 \left(\frac{\overline{u}\hat{\beta}}{\overline{T}} + \frac{\overline{\mu}\lambda^{*2}}{\Gamma^*}\right) - \frac{K\overline{u}\,\overline{u}y}{\overline{T}^2}\left(\frac{\overline{u}\hat{\beta}}{\overline{T}} + \frac{\overline{\mu}\lambda^{*2}}{\Gamma^*}\right) + \frac{K\overline{u}^2\overline{T}y}{2\overline{T}^3}\left(\frac{\overline{u}\hat{\beta}}{\overline{T}} + \overline{\mu}\lambda^{*2}\right) = 0, \quad (8.1)$$

and $\hat{\beta}$ is a maximum at $y = y_c$ where (8.1) is satisfied. Here $\overline{\mu}$ is the viscosity of the fluid and Γ^* is the Prandtl number. In the incompressible limit (8.1) reduces to precisely the expression given by DHS for the corresponding incompressible problem. We consider solutions of (8.1) when the basic flow is given by the compressible Blasius flow described by (2.4 - 7) for unit Chapman constant and Prandtl number. Then the situation of $\lambda^* = 0$ is precisely (6.3), determining the growth rate of the trapped layer mode. Thus, for $\lambda^* = 0$ there will not be a solution of (8.1) for values of M_∞ below a certain value. However, for $\lambda^* > 0$ we find that solutions of (8.1) exist for all values of M_∞. We are not concerned with the details of the solution of (8.1) here but further particulars may be obtained, on request, from the second author. We are solely concerned with the behavior of the solution of (8.1) for $\lambda^* \to 0$ for the basic flow described in Section 2. The numerical solutions of (8.1) show

that η_c becomes small for $\lambda^* \to 0$ and closer inspection of (8.1) in this limit reveals that $\eta_c \sim \lambda^{*4}$ and $\hat{\beta} \sim \lambda^{*-2}$. Thus, in the limit $\lambda^* \to 0$ the growth rates of the viscous modes are $0(G^{\frac{1}{2}}(aG^{-\frac{1}{4}})^{-2})$. Thus, as a decreases the viscous right-hand branch modes become more unstable.

The above discussion suggests that there exists an intermediate region where the viscous mode described above and the inviscid mode of Section 6 overlap. This will occur when their growth rates are the same size. We find that this is the case when $a \sim G^{\frac{1}{5}}$ with the growth rates of $0(G^{\frac{3}{5}})$. The vortices in this case will be confined to a wall layer of depth of $0(G^{-\frac{1}{5}})$. We note that this situation is identical to that described by DHS for the fastest growing mode in an incompressible flow. It turns out that the effects of compressibility may be scaled out with the result that the eigenvalue problem determining the growth rate of the fastest growing mode is identical to that solved by DHS. Thus we do not present the system of equations here but point out that full details of the compressible problem may be obtained from the second author. Consequently, the results of DHS also describe the solution for a compressible fluid. We have that each unstable mode has its maximum growth rate occurring at a finite value of λ^*. DHS showed that the most unstable mode corresponds to $\tilde{\lambda} = 0.476$, $\tilde{\tilde{\beta}} = 0.312$ where $a = K^{\frac{1}{5}}\alpha^{\frac{2}{5}}T_w^{-\frac{3}{5}}\tilde{\lambda}G^{\frac{1}{5}}$ and the growth rate of the fastest growing mode is given by $G^{\frac{3}{5}}K^{\frac{3}{5}}\alpha^{\frac{1}{5}}T_w^{-\frac{3}{5}}\tilde{\tilde{\beta}}$. The results described above show that for a compressible fluid, as well as an incompressible fluid, the most unstable linear Görtler vortex at high Görtler numbers is viscous with wavenumber of $0(G^{\frac{1}{5}})$, rather than $0(G^{\frac{1}{4}})$, which is appropriate to the unstable modes close to the right-hand branch of the neutral curve. An important result is that the most unstable modes occur close to the wall. This suggests that significant coupling coefficients will be possible in the receptivity problem for the most unstable modes. This was shown to be the case for the incompressible problem by DHS and identical results for a compressible fluid may be inferred simply from the results of DHS. Of interest would be the behavior of the fastest growing mode in the hypersonic limit.

Acknowledgement

The authors would like to thank Professor P. Hall for many useful discussions on this work. Support for A. D. from SERC and ICASE is acknowledged.

References

[1] Abramowitz, M. and Stegun, I. A. (1964), Handbook of Mathematical Functions (National Bureau of Standards, Frankfurt).

[2] Blackaby, N., Cowley, S. and Hall, P. (1990), On the instability of hypersonic flow past a flat plate. ICASE Report No. 90-40, and to be submitted to J. Fluid Mech.

[3] Cowley, S. and Hall, P. (1990), On the instability of the hypersonic flow past a wedge. J. Fluid Mech., **214**, 17-42.

[4] Denier, J. P., Hall, P. and Seddougui, S. O. (1991), On the receptivity problem for Görtler vortices and vortex motions induced by wall roughness. Phil. Trans. R. Soc. Lond. A, **335**, 51-85, and ICASE Report No. 90-31.

[5] Fu, Y., Hall, P. and Blackaby, N. (1990), On the Görtler instability in hypersonic flows: Sutherland law fluids and real gas effects. ICASE Report No. 90-85, and to appear in Proc. R. Soc. Lond. A.

[6] Hall, P. (1982a), Taylor-Görtler vortices in fully developed or boundary layer flows: linear theory. J. Fluid Mech., **124**, 475-494.

[7] Hall, P. (1982b), On the nonlinear evolution of Görtler vortices in growing boundary layers. J. Inst. Maths. and Applications, **29**, 173-196.

[8] Hall, P. (1983), The linear development of Görtler vortices in growing boundary layers. J. Fluid Mech., **130**, 41-58.

[9] Hall, P. (1990), Görtler vortices in growing boundary layers: the leading edge receptivity problem, linear growth and the nonlinear breakdown stage. Mathematika, December 1990, and ICASE Report No. 89-81.

[10] Hall, P. and Fu, Y. (1989), On the Görtler vortex instability mechanism at hypersonic speeds. Theoret. Comput. Fluid Dynamics, **1**, 125-134.

[11] Hall, P. and Malik, M. (1989), The growth of Görtler vortices in compressible boundary layers, J. Eng. Math., **23**, 239-251.

[12] Mack, L. M. (1987), Review of linear stability theory. In "Stability of Time Dependent and Spatially Varying Flows." (eds. D. L. Dwoyer and M. Y. Hussaini), Springer.

[13] Smith, F. T. and Brown, S. N. (1990), The inviscid instability of a Blasius boundary layer at large values of the Mach number. J. Fluid Mech., **219**, 499-518.

[14] Spall, R. E. and Malik, M. R. (1989), Görtler vortices in supersonic and hypersonic boundary layers. Phys. Fluids A, **1**, 1822.

[15] Stewartson, K. (1964), The Theory of Laminar Boundary Layers in Compressible Flows. Clarendon Press, Oxford.

[16] Wadey, P. (1990), Görtler vortices in compressible boundary layers. Exeter University, Ph.D. thesis, and to appear in J. Eng. Math.

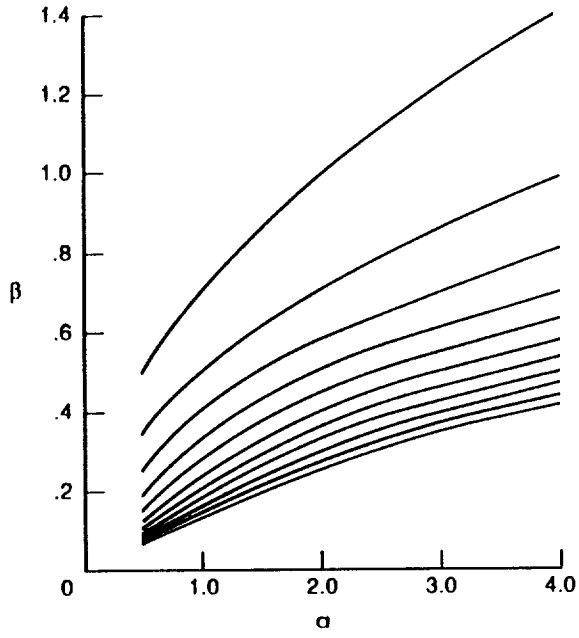

Figure 1. Solutions of the eigenvalue problem (2.16) - (2.17) for a Mach number of 2.

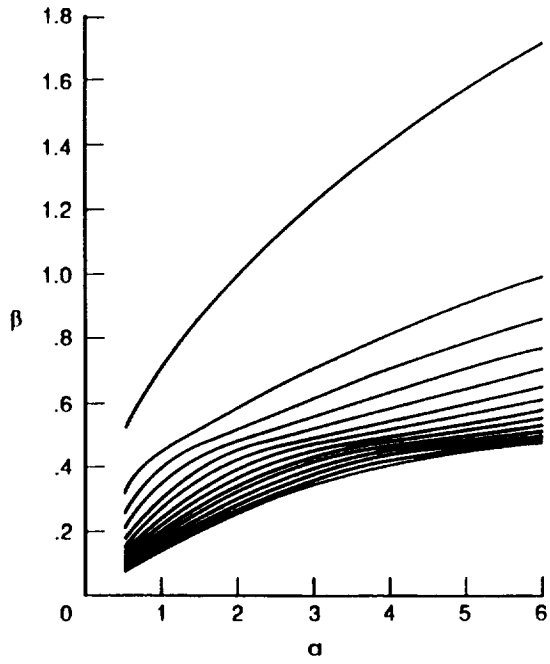

Figure 2. Solutions of the eigenvalue problem (2.16) - (2.17) for a Mach number of 3.25.

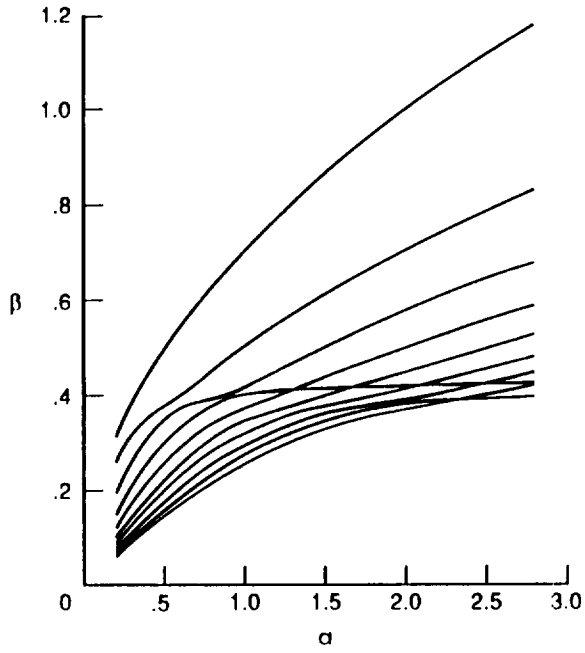

Figure 3. Solutions of the eigenvalue problem (2.16) - (2.17) for a Mach number of 5.

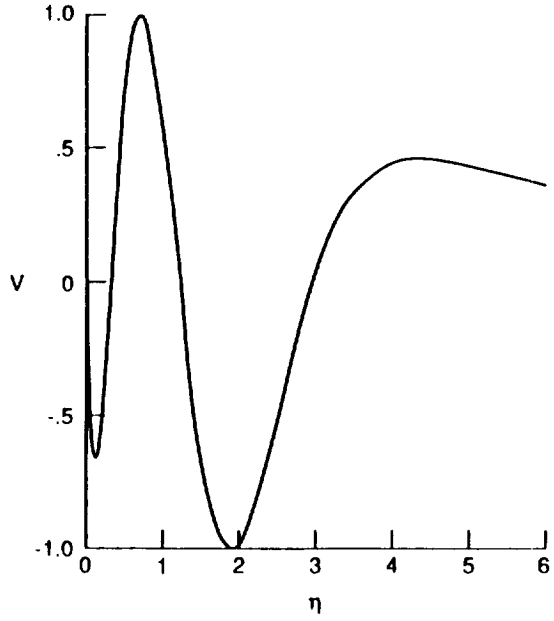

Figure 4a. Eigenfunction of the fourth mode for a Mach number of 5 and $a = 0.2$.

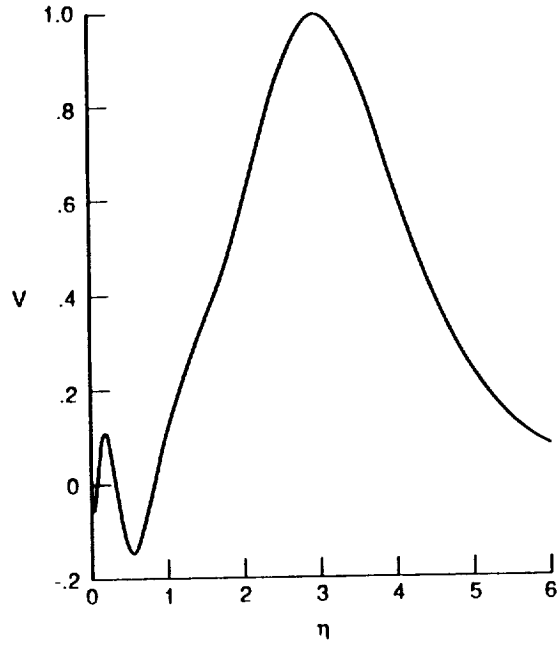

Figure 4b. Eigenfunction of the fourth mode for a Mach number of 5 and $a = 1.1$.

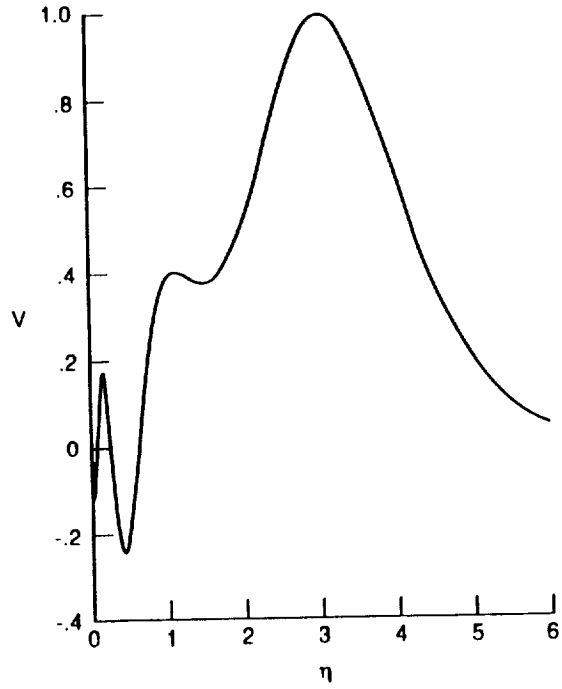

Figure 4c. Eigenfunction of the fourth mode for a Mach number of 5 and $a = 1.25$.

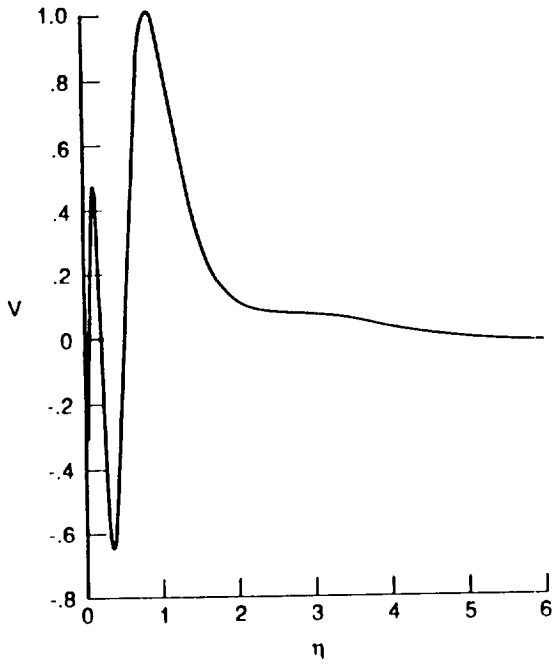

Figure 4d. Eigenfunction of the fourth mode for a Mach number of 5 and $a = 1.35$.

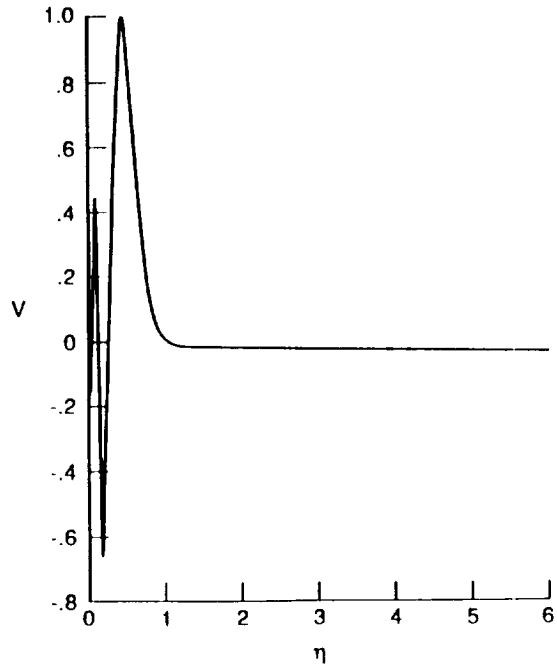

Figure 4e. Eigenfunction of the fourth mode for a Mach number of 5 and $a = 2.5$.

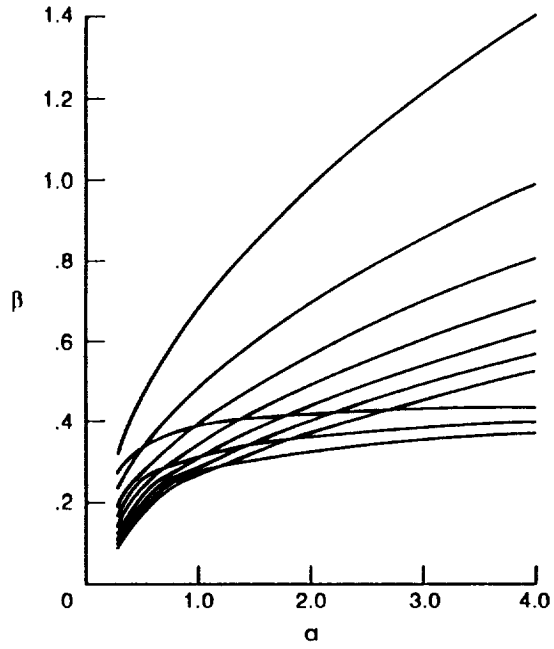

Figure 5. Solutions of the eigenvalue problem (2.16) - (2.17) for a Mach number of 8.

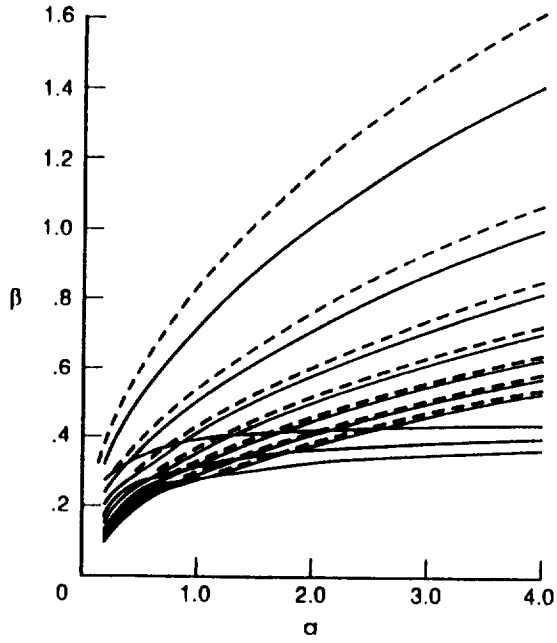

Figure 6. The first seven wall layer modes given by (3.17) for a Mach number of 8 (dashed lines) superimposed on Figure 5.

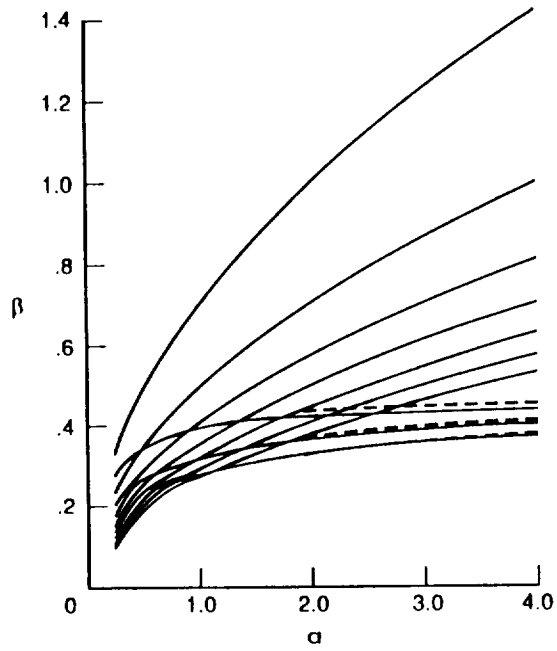

Figure 7. The first three adjustment layer modes given by (4.19) for a Mach number of 8 (dashed lines) superimposed on Figure 5.

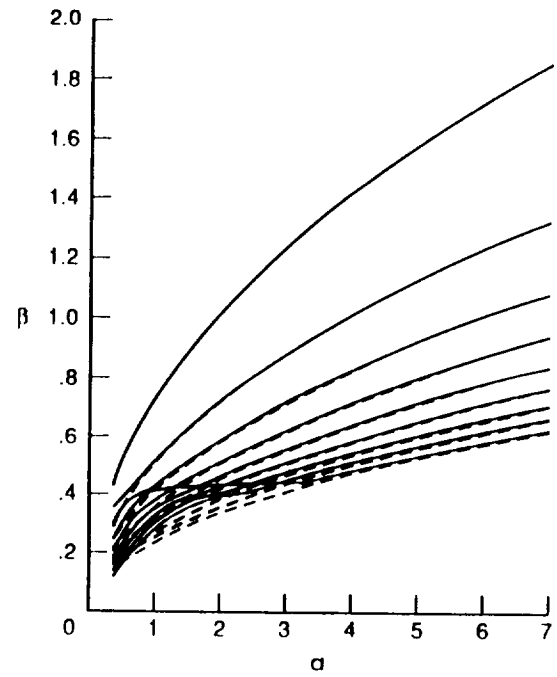

Figure 8. The growth rate β as a function of a for $M_\infty = 5$: — numerical solution of (2.16); – – – asymptotic solution from (5.4).

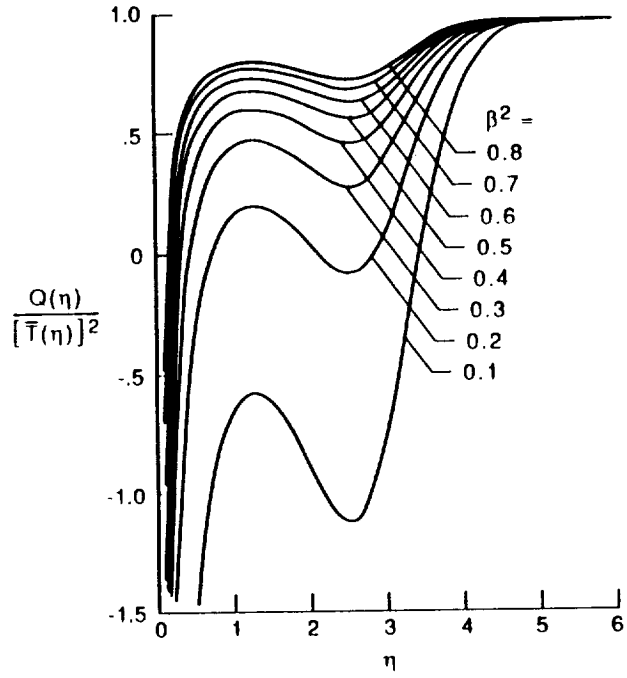

Figure 9. The function $Q(\eta)/[\overline{T}(\eta)]^2$ from (6.2) for a range of values of β for $M_\infty = 5$.

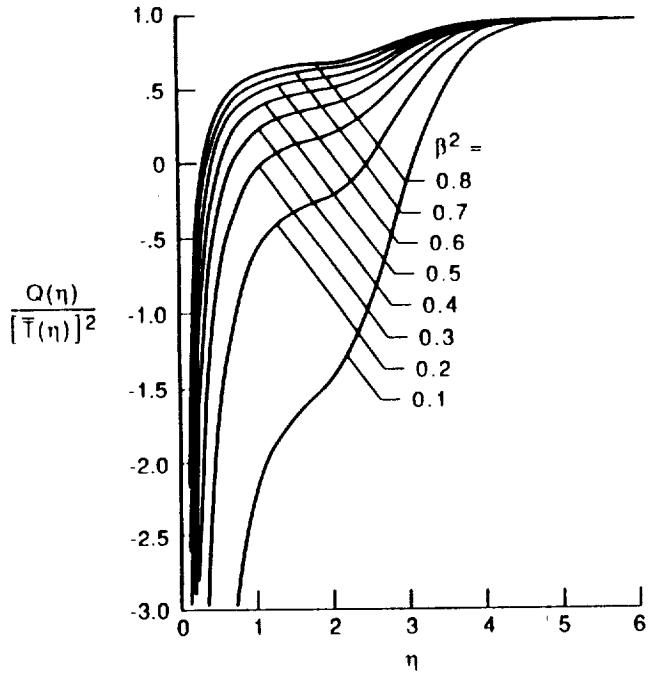

Figure 10. The function $Q(\eta)/[\overline{T}(\eta)]^2$ from (6.2) for a range of values of β for $M_\infty = 3$.

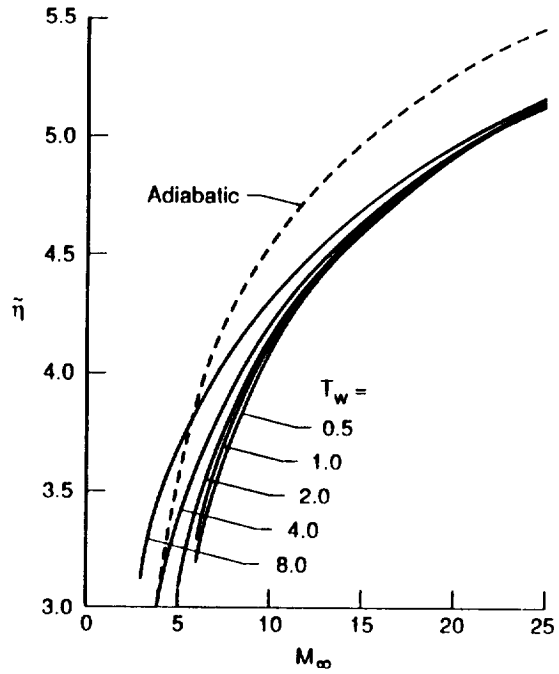

Figure 11. The position $\tilde{\eta}$ of the trapped layer modes for $a \gg 1$ as a function of M_∞ for an adiabatic fluid and also for an isothermal fluid with $T_w = 0.5, 1, 2, 4, 8$.

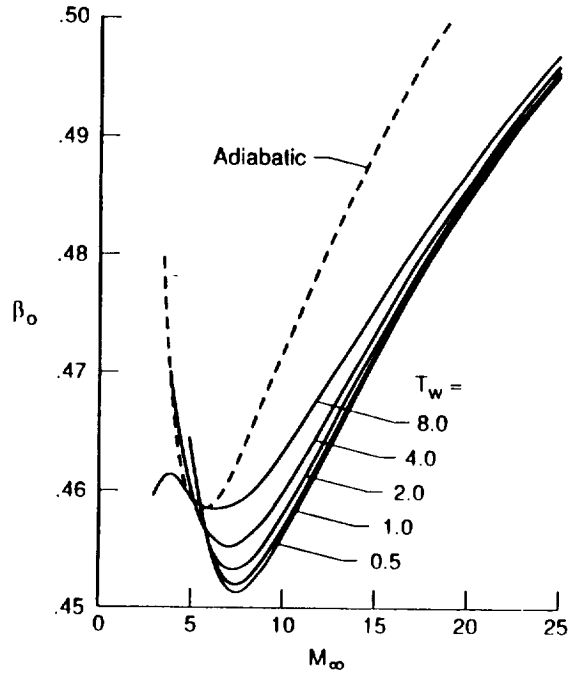

Figure 12. The neutral growth rate β_0 from (6.3) for the trapped layer modes as a function of M_∞ for an adiabatic fluid and also for an isothermal fluid with $T_w = 0.5, 1, 2, 4, 8$.

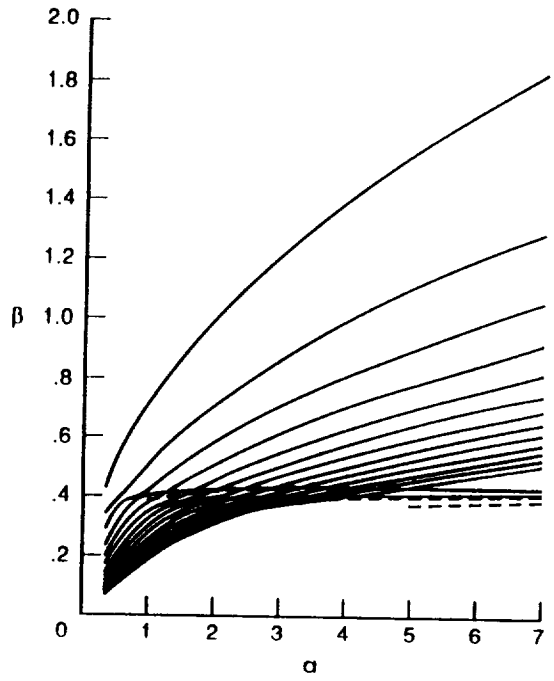

Figure 13. The growth rate β as a function of a for $M_\infty = 5$: — numerical solution of (2.16); – – – asymptotic solution from (6.6).

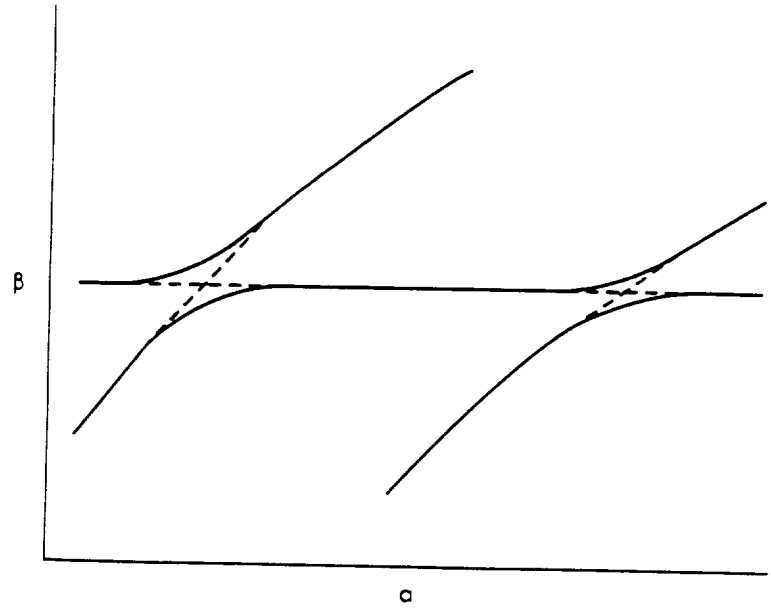

Figure 14. Sketch of the near crossing of the wall layer and adjustment layer modes. The continuous curves represent the finite Mach number situation and the dashed lines the situation in the asymptotic limit $M_\infty \to \infty$.

Report Documentation Page

NASA
National Aeronautics and Space Administration

1. Report No.	2. Government Accession No.	3. Recipient's Catalog No.
NASA CR-187600 ICASE Report No. 91-54		

4. Title and Subtitle	5. Report Date
THE INVISCID COMPRESSIBLE GÖRTLER PROBLEM	July 1991
	6. Performing Organization Code

7. Author(s)	8. Performing Organization Report No.
Andrew Dando Sharon O. Seddougui	91-54
	10. Work Unit No.
	505-90-52-01

9. Performing Organization Name and Address	11. Contract or Grant No.
Institute for Computer Applications in Science and Engineering Mail Stop 132C, NASA Langley Research Center Hampton, VA 23665-5225	NAS1-18605
	13. Type of Report and Period Covered
	Contractor Report

12. Sponsoring Agency Name and Address	14. Sponsoring Agency Code
National Aeronautics and Space Administration Langley Research Center Hampton, VA 23665-5225	

15. Supplementary Notes

Langley Technical Monitor:
Michael F. Card

To be submitted to IMA Journal of Applied Mathematics

Final Report

16. Abstract

In this paper we investigate the growth rates of Görtler vortices in a compressible flow in the inviscid limit of large Görtler number. Numerical solutions are obtained for O(1) wavenumbers. The further limits of (i) large Mach number and (ii) large wavenumber with O(1) Mach number are considered. We show that two different types of disturbance modes can appear in this problem. The first is a wall layer mode, so named as it has its eigenfunctions trapped in a thin layer away from the wall and termed a trapped layer mode for large wavenumbers and an adjustment layer mode for large Mach numbers, since then this mode has its eigenfunctions concentrated in the temperature adjustment layer. We are able to investigate the near crossing of the modes which occurs in each of the limits mentioned.

17. Key Words (Suggested by Author(s))	18. Distribution Statement
Inviscid Görtler Instability; compressible flows	02 - Aerodynamics 34 - Fluid Mechanics and Heat Transfer Unclassified - Unlimited

19. Security Classif. (of this report)	20. Security Classif. (of this page)	21. No. of pages	22. Price
Unclassified	Unclassified	40	A03

NASA FORM 1626